NISTIR 4405

Models of Transport Processes in Concrete

U.S. Department of Commerce
National Institute of Standards and Technology
Center for Building Technology
Gaithersburg, MD 20899

Prepared for:
U.S. Nuclear Regulatory Commission
Office of Nuclear Regulatory Research
Division of Engineering
Washington, DC 20555

NISTIR 4405

Models of Transport Processes in Concrete

James M. Pommersheim*
James R. Clifton

*Chemical Engineering Department
Bucknell University
Lewisburg, PA 17837

September 1990

U.S. Department of Commerce
Robert A. Mosbacher, *Secretary*
National Institute of Standards and Technology
John W. Lyons, *Director*
Center for Building Technology
Gaithersburg, MD 20899

Prepared for:
U.S. Nuclear Regulatory Commission
Office of Nuclear Regulatory Research
Division of Engineering
Washington, DC 20555

EXECUTIVE SUMMARY

The U.S. Nuclear Regulatory Commission (NRC) has the responsibility for developing a strategy for the disposal of low-level radioactive waste (LLW). An approach being considered for their disposal is to place the waste forms in concrete vaults buried in the earth. A service life of 500 years is required for the concrete vaults as they may be left unattended for much of their lives.

In order to provide a basis for making predictions of service life, mathematical models for the important transport processes which occur during cement and concrete degradation processes were developed. The method of dimensionless groups was first used to determine the relative importance of the possible rate-controlling processes. These included diffusion, convection, reaction and sorption of chemical species. Based on rate laws for these phenomena, general conservation equations were developed and applied to three processes: the penetration of chloride ions through concrete, acid attack or leaching, and the penetration and reaction of sulfate ions in concrete. The models formulated were solved analytically to predict concentration profiles within the concrete and, in some cases, the location of the reaction front or deterioration zone. For each model the key dimensionless groups were identified and their effect on the model solution was determined. For chloride ion intrusion, concentration varied with both time and position within the concrete as a result of diffusion and reaction or sorption. Reactions between chloride ion and hydrated tricalcium aluminate were considered. The model for acid attack involved the penetration of dissolved carbon dioxide, carbonic acid or bicarbonate ion into the concrete to react with alkali hydroxides and calcium hydroxide. Both reaction and diffusion-controlled limit solutions were developed. The model developed for sulfate attack involved a moving interface between a porous or cracked ettringite-rich layer near the outside of the exposed concrete and a relatively impermeable monosulfate-rich layer on the inside. At the moving front, soluble sulfate, brought in from the outside by diffusion and convection, rapidly converted monosulfate to expansive ettringite. Both co-current and counter-current flow were examined. Counter-current flow (in the direction opposing diffusion) slows the progress of the deteriorated zone, and thus extends service life. These models, when validated against experimental data, can form the basis for predicting the life of concrete under in-service conditions.

ABSTRACT

An approach being considered by the U.S. Nuclear Regulatory Commission for disposal of low-level radioactive waste is to place the waste forms in concrete vaults buried underground. The vaults would need a service life of 500 years. Approaches for predicting the service life of concrete of such vaults include the use of mathematical models.

Mathematical models are presented in this report for the major degradation processes anticipated for the concrete vaults, which are corrosion of steel reinforcement, sulfate attack, acid attack, and leaching. The models mathematically represent rate controlling processes including diffusion, convection, and reaction and sorption of chemical species. These models can form the basis for predicting the life of concrete under in-service conditions.

KEYWORDS: Acid attack; chloride; concrete; convection; corrosion; degradation; diffusion; leaching; mathematical model; service life; sulfate attack; transport processes.

Table of Contents

Table of Contents (continued)

LIST OF FIGURES

LIST OF TABLES

1. INTRODUCTION

The U.S. Nuclear Regulatory Commission has the responsibility for developing a strategy for disposing of low-level radioactive wastes. According to one approach, the radioactive wastes would be placed in concrete vaults which are either buried in the earth or constructed above ground and covered with earth. A service life of 500 years is required for the storage vaults. The National Institute of Standards and Technology is carrying out a project aimed at developing performance criteria for concrete used in constructing the vaults. Criteria are being developed based on service life predictions which take into consideration processes that are likely to degrade concrete located underground.

The major degradation processes that the reinforced concrete is likely to encounter have been previously identified [1] to be sulfate attack, corrosion of reinforcing steel, alkali-aggregate reactions, and leaching by percolating water. These degradation processes involve ingress and movement of moisture in concrete, through convection or capillary forces. Soluble salts and dissolved gases are transported into concrete by the movement of moisture and by diffusion. Therefore, the rates of the degradation

processes are dependent on the rates of intrusion of moisture and dissolved salts and gases.

This report describes models of diffusion and convection processes developed to predict the rates of intrusion of moisture and dissolved salts and gases into concrete. In future work, these models will be linked with macromodels for predicting service lives of concrete.

2. CONCEPTUAL MODELS FOR TRANSPORT PROCESSES

2.1 Diffusion and Convection

Figure 1 is a schematic diagram of a concrete member or slab in which diffusion (driven by concentration differences ΔC) and convection or flow (driven by pressure differences, ΔP) are the principal transport processes. In this schematic both processes drive the penetrant through the slab in the same direction, i.e., co-currently. Countercurrent flow occurs when convection and diffusion oppose one another. Within the slab, sorption processes (adsorption and absorption) and reaction mechanisms (hydration and reaction of penetrants with concrete constituents) can also be present. The pores of the slab are assumed to be initially saturated with water which is free of dissolved salts and gases. Except under very dry external conditions, this is a

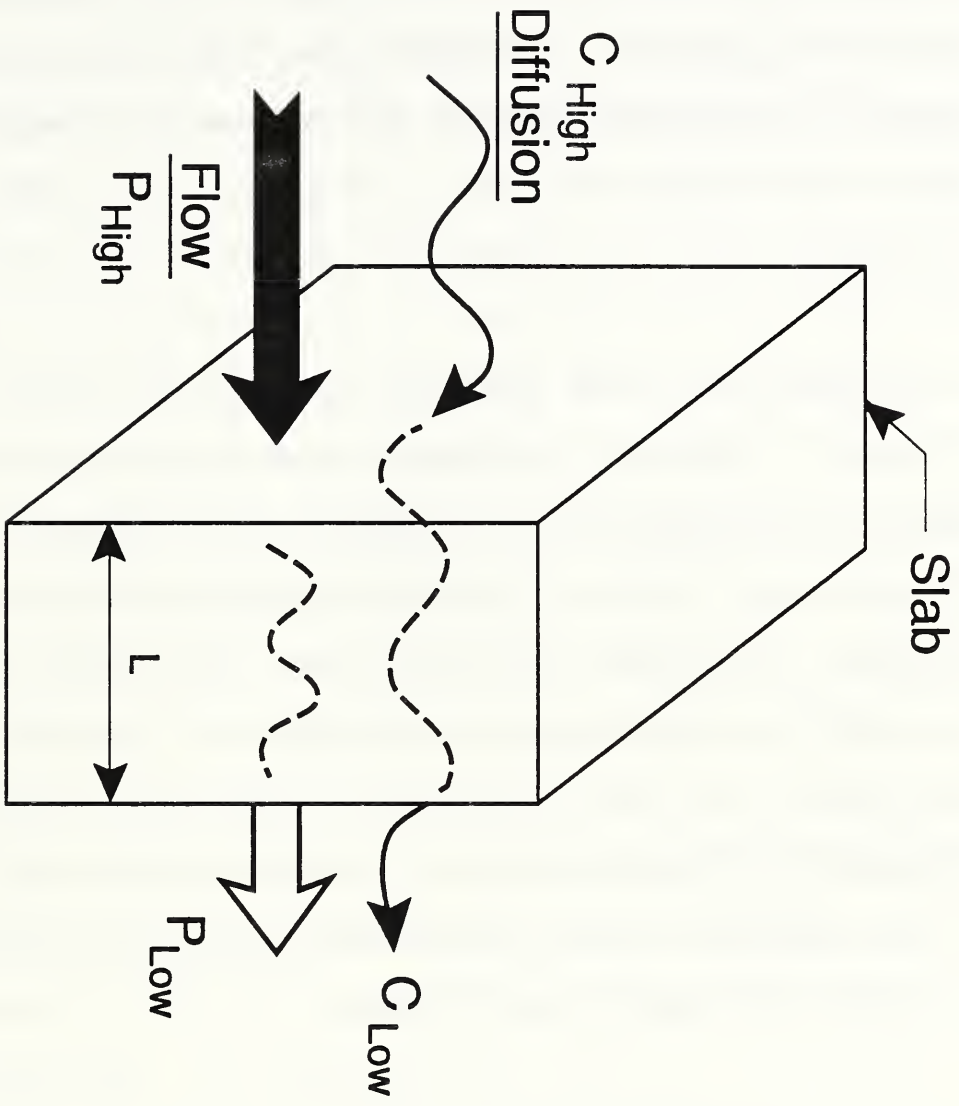

Figure 1. Physical model of section of concrete element.

reasonable scenario.

The relative importance of the processes depends on both external factors, such as concentration and pressure gradients, specimen size and shape, and temperature; and internal or microstructural factors, such as phase composition, pore structure, and permeability of the concrete.

The dependence of the transport processes on the pore size is shown in Table 1. Diffusion and convection are the dominant phenomena in the larger (macro) pores with diffusion and surface phenomena (sorption and reaction) important in smaller (micro) pores. The small and large pores can be interconnected and pores of intermediate size also exist, but such a macropore-micropore model is not unnecessarily complex since, in the mathematical formulation of the problem, molar conservation equations do not need to be solved for every size of pore.

2.2 Method of Dimensionless Groups

Most realistic models for transport of penetrants through porous materials are complex. Even those which treat only one or two pore sizes will involve the solution of coupled partial differential equations. However considerable initial insight into the nature of the controlling

mechanisms can be gained using the method of dimensionless groups without the immediate need to solve such equations.

In this method, dimensionless groups are formed as ratios (R) of the rates of important phenomena. Table 2 presents some common dimensionless groups for phenomena which can be present in cementitious systems. Let R' = x/y, where x and y are two different transport processes. If the ratio is high and the two phenomena are in parallel, then phenomenon x, the fast step, controls the overall rate. An example would be diffusion and convection in porous media, such as illustrated in Figure 1. Here the key dimensionless group is the Peclet number (Pe) defined as:

$$Pe = \epsilon vL/D_e \qquad (1)$$

where ϵ is the (flow) porosity, v is the average convective flow velocity within the slab, L the slab thickness, and D_e is the effective diffusion coefficient through the porous medium of the slab. In terms of the ratio R', x is the convection rate v, and y is the diffusion rate $D_e/\epsilon L$. Since these phenomena are in parallel, if $x >> y$, convection controls.

For processes in series, the slow process controls the overall transport rate. An example is diffusion (y) to a solid-fluid interface where a surface process (x), such as

Table 1. Effect of Pore Size on Transport Processes

Phenomenon	Large Pores	Small Pores
Diffusion	X[a]	X
Convection	X	
Reaction		X
Sorption		X

[a]X indicates potentially important phenomenon.

Table 2. Dimensionless Groups Used in Models

Time Ratio (diffusion)	$\frac{tD_e}{L^2\epsilon}$	$\frac{\text{actual time}}{\text{diffusion time}}$
Time Ratio (convection)	$\frac{tv}{L}$	$\frac{\text{actual time}}{\text{convection time}}$
Peclet Number	$\frac{vL\epsilon}{D_e}$	$\frac{\text{convection rate}}{\text{diffusion rate}}$
Sorption Modulus	$\frac{k_aL}{D_e}$	$\frac{\text{sorption rate}}{\text{diffusion rate}}$
Reaction Modulus	$\frac{kR}{D_e}$	$\frac{\text{reaction rate}}{\text{diffusion rate}}$
Thiele Modulus	$\left[\frac{k'R^2}{D_e}\right]^{1/2}$	$\frac{\text{reaction rate}}{\text{diffusion rate}}$

chemical reaction, occurs. Now if R' = x/y is high, the slow process (diffusion) controls the reaction rate. The reaction modulus is the name given to R' in this situation. As an example, in modeling tricalcium silicate hydration, Pommersheim and Clifton [2] used a similar reaction-diffusion modulus defined as kR/D_e, where k is the reaction velocity constant and R the initial particle radius. They assumed that a first order surface reaction occurred at the interface between the first hydrate layer and the unreacted particle core. At high values of this modulus they found that diffusion controlled the hydration rate, while at low values, it was reaction controlled. For reactions in which there is a moving interface, the modulus is more properly defined as kw/D_e, where w is the thickness of the reaction rim which has formed. In chemical reactor theory such a group is termed the Damkohler number [3]. When reaction occurs throughout the bulk of a porous material, as in many heterogeneous chemical reactions, the appropriate dimensionless group to use is the Thiele modulus, which is $[k'R^2/D_e]^{1/2}$ for a first order chemical reaction with reaction velocity k' [3].

Table 2 also presents dimensionless time ratios, which give a measure of how important transient effects are in cementitious systems. Consider the time ratio $(tD_e/\epsilon L^2)$: it is the ratio of the test duration (t) to the time taken for another process which is considered important, in this case,

diffusion. The diffusion time t_d equals $\epsilon L^2/D_e$. The criterion for the attainment of a large fraction of steady state is that the duration t be much greater than the diffusion time t_d, i.e., $t >> t_d$. For example, consider a concrete slab in which it has been shown that diffusion is an important phenomenon. In this example the slab has L = 2 cm, ϵ=0.2, and $D_e = 2 \times 10^{-12}$ m^2/s. These values of porosity and diffusivity are typical of those observed in hardened cement pastes [3]. To determine if steady state has been achieved in one year (3×10^7s) the calculation is:

$$t_d = \frac{4 \text{ cm}^2 \times 0.2}{2 \times 10^{-12} \text{ m}^2/\text{s}} \times \frac{\text{m}^2}{(100 \text{ cm})^2} = 4 \times 10^7 \text{s} \qquad (2)$$

Since t_d is of comparable magnitude to t, a steady state was not attained in this example even after a year. In fact it would take over five years for steady state to be approached. If it has been shown by the method of dimensionless ratios that convection is a more important phenomenon than diffusion, then the proper time ratio is t/t_c, where $t_c = L/v$ is the convective time. In this case steady state will be reached when $t >> t_c$.

In summary, these results show that it may take months to reach an appreciable fraction of steady state, even for thin walls. For diffusion controlled processes, it is the very small diffusion coefficients through hardened cement pastes

which lead to this conclusion. In applying this criterion, it is important to compare the duration of exposure to the time for the correct controlling phenomenon. This is explored further in the next section where diffusive and convective phenomena are compared.

2.3 Diffusion vs. Convection in Cementitious Systems

A method is presented in this section to determine if convection or diffusion is likely to be the rate controlling process for transport in concrete. Qualitatively, diffusion will control if there are many small pores, while convection will control if there are a number of large pores. The way to estimate how small is "small" is to use the Peclet number (Pe), the dimensionless ratio of the convection rate to the diffusion rate. When this ratio is equal to unity, convection and diffusion will occur with nearly equal rates.

As a system consider a single pore of radius r and length L through which fluid moves with average velocity v. The appropriate Peclet number is vL/D where D is the free stream (unhindered) diffusivity of the transported species. The average velocity of flow, v, can be eliminated from the Peclet number using Poiseuille's law:

$$v = \frac{(\Delta P/L)\ r^2}{8\mu} \qquad (3)$$

where $\Delta P/L$ is the pressure gradient across the pore, and μ is the viscosity of the flow medium. The assumption of laminar flow, implicit in this relation, is assured considering the small pore sizes that occur within concrete. Solving for the critical pore radius r* where convection and diffusion are of equal importance (Pe = 1):

$$r^* = \left[\frac{8\mu D}{\Delta P}\right]^{1/2} \qquad (4)$$

Table 3 indicates the effect that cement pore size has on whether diffusion or convection controls transport. In this table the actual value of the average pore radius (r) is compared to the critical pore radius (r*) to determine the controlling mechanism. When the Peclet number is much less than unity, diffusion controls and most pores are smaller than r*. When most pores are about the size of r*, neither mechanism will control transport. Note that r* is independent of slab thickness L. For liquids the product μD is only a function of temperature and intermolecular interactions. It decreases with increasing temperature. For gases, the μD product varies directly with temperature and inversely with pressure [4]. The average pressure across the slab should be used in gas phase calculations of

the diffusivity. For liquids $\mu \simeq 1$ cp and $D \simeq 2 \times 10^{-5}$ cm^2/s. This makes r* a function of only one variable, the external pressure difference ΔP. Thus, for typical values of ΔP, r* can be calculated and compared to experimental data.

Table 4 shows the results of such calculations. As ΔP goes from 1 atm to 0.001 atm (1000 cm H_2O to 1 cm H_2O), r* goes from 12.4 nm to 400 nm as the controlling mechanism shifts from convection to diffusion. Note that for $\Delta P = 0$, there would be no convection, and diffusion would always control. This is confirmed since, at suitably low values of ΔP, r*, from equation (4) takes on values which will be greater than any of the actual pore sizes. It is important to mention that when pressure differences due to hydrostatic forces are also present, that these must be added to ΔP in order to give an effective total driving force or head due to both pressure and gravity.

Pore size distribution data for hardened portland cement paste (HCP) are usually obtained by mercury intrusion porosimetry (MIP). Figure 2 shows data obtained by Kumar [5] for HCP at a water to cement ratio (w/c) of 0.3. Most pores lie in the range from 6 to 20 nm. For a given ΔP across the slab this range can be compared to r*. When ΔP = 1 atm, r* = 12.4 nm. As shown in the figure, this value of r* lies in the middle of the range of most pores, indicating

Table 3. Effect of Cement Pore Size on Controlling Mechanism in Cementitious Systems

Cement Pore Size[a]	Controlling Mechanism	Peclet Number
$r >> r^*$[b]	convection	$Pe >> 1$
$r \simeq r^*$	neither controls	$Pe \simeq 1$
$r << r^*$	diffusion	$Pe << 1$

[a]predominant number of pores

[b]critical pore radius

Table 4. Effect of Pressure Change (ΔP) on Controlling Mechanism in Cementitious Systems

ΔP		r^*[a]	controlling
atm	mm H_2O	nm	mechanism
4.0	40000	6.2	convection
1.0	10000	12.4	
0.1	1000	40	mixed control
0.01	100	124	
0.001	10	400	diffusion

[a]critical pore radius.

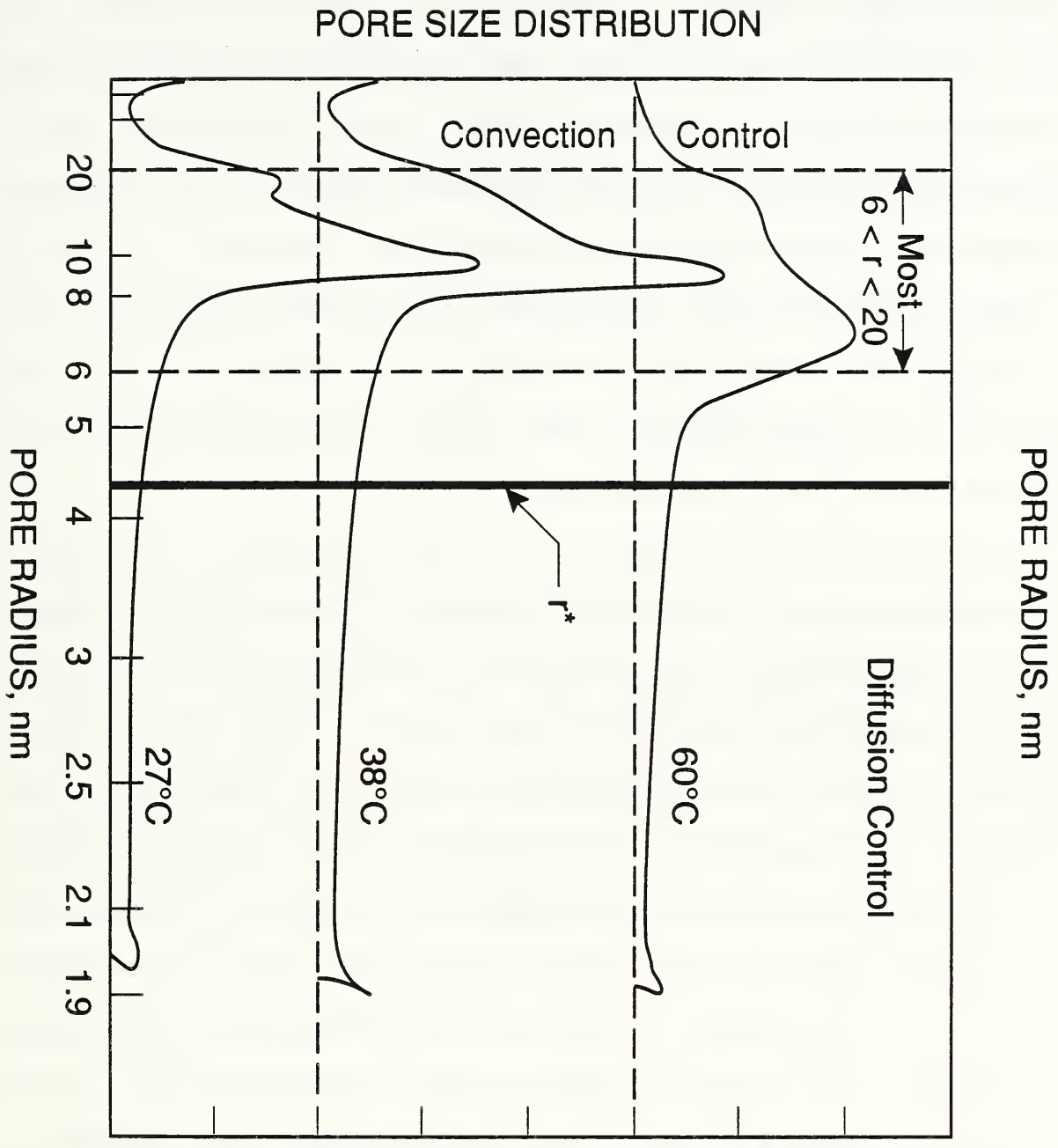

Figure 2. Pore size distribution of typical hardened portland cement paste: w/c ratio of 0.3; 0.33% superplasticizer [5].

that neither convection nor diffusion is controlling at that pressure difference. If ΔP = 0.01 atm, r^* = 62 nm, and most of the pores are smaller, indicating diffusion control. With ΔP = 8 atm, r^* = 4.4 nm, and convection is the dominant transfer mechanism. This is marked in the figure by the solid vertical line. Since a pressure drop of 8 atmospheres across the slab is unlikely, convection, by itself, would not be controlling for this paste. At higher values of w/c and at earlier ages, penetration is more likely to be convection controlled since the pores would normally be larger under these conditions.

As compared to portland cement paste, pores within concrete have a wider range, with many more large pores present. If there are cracks penetrating the concrete slab these can present a short circuit for flow, and to a lesser extent, diffusion. For example, it is easy to show using equation (3) that even a single microscopic crack having a size of 0.01 mm and passing completely through the slab will carry at least as much flow as six million continuous 200 nm macropores. With several such cracks, transport of deleterious species through concrete members will become convection controlled. This result shows the importance of preventing the formation of stress cracks in concrete members intended for use in storage facilities for LLW which are subject to hydraulic or pressure gradients.

Other studies have shown that MIP does not lead to an accurate description of pore sizes since it only gives the distribution of entry or neck pores. Dullien and coworkers [6,7] have shown that the pore size distribution of all pores, obtainable using photomicroscopy, is also needed in order to obtain a complete description of the permeability of the flow network. This distribution is usually flatter than that found using MIP, indicating that an appreciable fraction of larger pores may actually exist. This makes convection more likely to be a dominant mechanism.

In summary, convection can be an important mechanism for intrusion of penetrant, unless there are no pressure gradients, the pores are all small, or convection opposes diffusion (counter-current flow). In the last case, flow acts to prevent the penetrant from entering the concrete. In cases where the concrete is cracked, convection is much more likely to control intrusion rates of deleterious species. For this reason it is important to prevent the formation of stress cracks in concrete members. In addition, caution must be exercised in using pore sizes found from MIP data as the sole basis for determining the dominant transport mechanism.

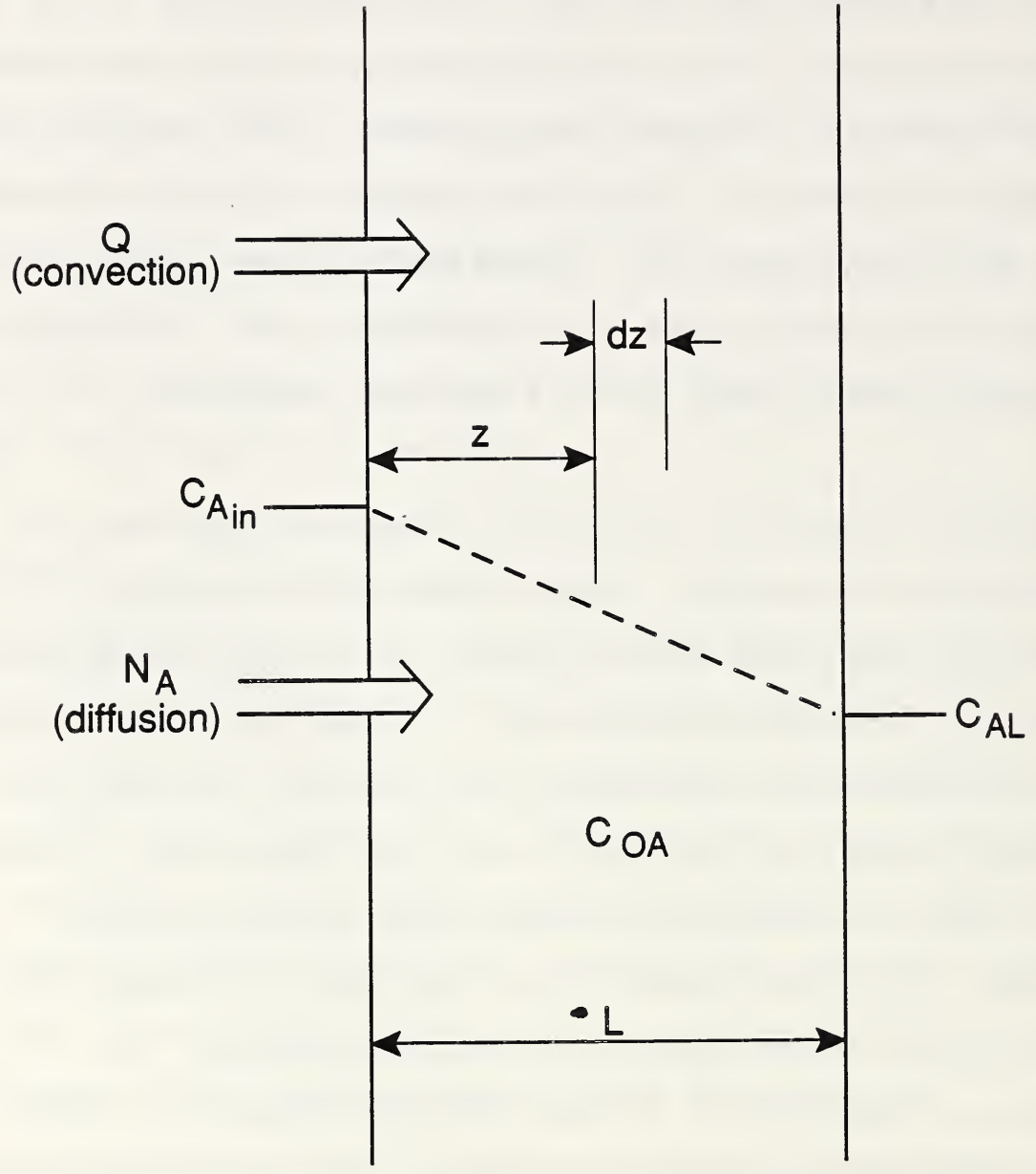

Figure 3. Model system for penetration of chemical species through porous material.

3. MATHEMATICAL MODELS

Although the method of dimensionless groups can provide valuable information about the controlling phenomena in cementitious systems it does not have as firm a quantitative basis as do the results of modeling studies. In this section mathematical models are developed for the intrusion of deleterious chemical species through concrete. The models incorporate diffusion, convection, reaction and sorption (adsorption and absorption) as important phenomena. They are based on rate laws for these phenomena and overall conservation equations for chemical species.

3.1 Model System

As illustrated by figure 3 the model system is a plane or slab of concrete which is exposed on one side to a high concentration $C_{Ain}(t)$ of ions of species A. In this system, the pores of the concrete remain saturated with liquid water throughout the penetration process. The concrete itself initially contains the ions at concentration $C_{OA}(z)$, while the far side of the specimen (at z=L) is at concentration $C_{AL}(t)$. Because the slab width is much larger than its thickness, transport occurs only in the z direction. As a result of the concentration gradient, ions diffuse into the slab. They can also be transported in by co-current flow of

the external solution; or, flow can oppose diffusion. With countercurrent flow the penetration is retarded, while with co-current flow, where diffusion and convection occur in the same direction, penetration is augmented.

3.2 Rate Law for Diffusion

The rate law for diffusion is Fick's first law:

$$N_A = -D_{eA} \left(\frac{\partial C_A}{\partial z}\right) \tag{5}$$

where N_A is the molar flux of A ($mol/m^2 \cdot s$), C_A is the concentration of A (mol/m^3) within the slab and D_{eA} is the effective diffusivity of A (m^2/s) through the pores of the concrete. Species A can be any compound, including, for example, dissolved carbon dioxide or ions such as chloride, sulfate or bicarbonate. The effective diffusion coefficient D_{eA} will be less than the ionic/molecular or free stream diffusivity D_A of ions and molecules moving unimpeded through a bulk solution. For gases in very fine pores, transport more likely occurs by collision with the walls rather than by collisions with other molecules and the diffusion coefficient used should be the Knudsen diffusivity [3]. In a liquid system, Knudsen diffusion is unlikely since molecular collisions are more frequent.

The diffusion of ions and molecules in concrete is slowed because:

1) the effective area of diffusion is lowered due to the presence of the solid phase.

2) the diffusion path is tortuous so that it takes longer for molecules to pass from one point to another.

3) any given diffusion path has constricted regions (bottlenecks) where there is a greater resistance to the diffusive flow of molecules.

4) the connectivity of the pores is not complete.

The effects of these constraining factors are mathematically expressed in the relationship [8]:

$$D_{eA} = D_A \epsilon \frac{\sigma}{\tau} \qquad (6)$$

The porosity ϵ (volume fraction pores) and constriction factor σ are both less than unity, while the tortuosity t is greater than unity. All three factors act to lower the effective diffusion coefficient D_{eA} relative to its free stream value D_A. In general, equation (6) cannot be used to predict the value of D_{eA} since the geometric factors, σ and

τ are complicated functions of the pore structure. As an example, Bruggeman [9] has shown theoretically, using an electrical analog model, that σ/τ varies approximately as $\epsilon^{1/2}$. Based on equation (6), then, the diffusion coefficient should vary as $\epsilon^{3/2}$. However, the useful range of Bruggeman's approximation is only from $0.4 < \epsilon < 1$, which is outside the range of most concretes. At lower porosities, the dependence of effective diffusivity on porosity is even more pronounced than $\epsilon^{3/2}$, although the actual dependence has not been determined theoretically.

3.3 Rate Law for Convection

The rate law for convection is:

$$F_A = C_A Q = C_A v S \epsilon \qquad (7)$$

where F_A is the molar flow rate of A (mol/s) through the porous media, Q (m^3/s) is the volumetric flow rate and S is the total cross section. The porosity ϵ must be introduced since the flow average velocity v is based on the available flow area. In equation (7) it is presumed that there is only one velocity. This is a reasonable assumption considering that the porous media breaks up the flow and tends to make it uniform across the cross section. However, if the pores do not have a narrow pore size distribution centered around an average pore size, such an approximation

will be less likely to be valid, since, as discussed in Section 2, the larger pores will carry a disproportionately higher part of the flow.

3.4 Rate Laws for Reaction and Sorption

In addition to the mechanisms of diffusion and convection, mass transfer of deleterious chemical species is also influenced by the rates at which species are removed from solution by sorption (adsorption and absorption) and chemical reaction. Adsorption and chemical reaction are both surface phenomena which occur on the walls of the pores. Let $-r_A$ be the sorption or reaction rate of chemical A per unit of pore surface area ($mol/m^2 \cdot s$). In general:

$$-r_A = k\ f(C_i) \tag{8}$$

where k is the sorption or reaction rate constant and $f(C_i)$ is a kinetic function of reactant and product concentrations. The minus sign indicates that species A is disappearing from solution. Often the kinetics of sorption or reaction is unknown. In this case separate experiments must be conducted in the absence of diffusive and convective gradients to obtain data from which the rate law can be deduced.

3.4.1 Chemical Reaction Rate Laws

For chemical reactions:

$$aA + bB = uU + yY \tag{9}$$

where a, b, u, and y are stoichiometric coefficients, respectively, for chemicals A, B, U and Y, equation (8) often takes the general form:

$$-r_A = k_1 C_A^a C_B^b - k_2 C_U^u C_Y^y \tag{10}$$

where k_1 and k_2 are the forward and reverse reaction velocity constants. K_r, the thermodynamic reaction equilibrium constant, is equal to k_1/k_2. For reactions which are not thermodynamically consistent, the reaction orders will not be equal to the stoichiometric coefficients.

For irreversible processes the reaction rate only depends on reactant concentrations. When one of the reactants is present in large molar excess or there is only one reactant, A, equation (10) reduces to:

$$-r_A = k_1 C_A^m \tag{11}$$

where m is the kinetic order of reaction with respect to reactant A. When the reaction order matches the stoichiometry, m = a.

3.4.2 Sorption Rate Laws

When adsorption and desorption occur within the pores of the concrete, the rate equation can take on a number of mathematical forms depending on the kinetics of sorption. The most widely used sorption rate law is the Langmuir equation given by:

$$- r_A = \frac{k_a \, C_A}{1 + K_a \, C_A} \qquad (12)$$

where $-r_A$ is the rate of adsorption ($mol/m^2 \cdot s$), and k_a is the adsorption rate constant. K_a is the adsorption equilibrium constant, equal to k_a/k_d, where k_d is the desorption rate constant.

Other sorption rate laws include the Freundlich, Temkin and Henry isotherms [10]. The type of isotherm depends on whether the adsorption is physical or chemical and on the precise mechanism of interaction between the adsorbing ions and the substrate. As an example, consider the Langmuir isotherm under the condition that the adsorbed species are only weakly held on the walls of the pores. Since

adsorption is the slow step, this is an adsorption controlled situation. In this case, surface coverage of adsorbed species will be low, $k_a << k_d$, the adsorption equilibrium constant K_a will be small, and $K_a C_A << 1$, so that equation (12) reduces to:

$$-r_A = k_A C_A \qquad (13)$$

This corresponds to the Henry isotherm. In this equation the adsorption rate is equivalent to that for a first order irreversible chemical reaction, i.e., m = 1 in equation (11).

When the adsorbed species are strongly held to the surface, the net rate of sorption will be desorption controlled. For this case, $K_a C_A >> 1$ and equation (12) reduces to:

$$- r_A = k_d \qquad (14)$$

which is equivalent to a zero order chemical reaction.

3.4.3 Effect of Temperature and Pressure

The kinetic rate constants for reaction (k_1 and k_2) and sorption (k_a and k_d) and the thermodynamic equilibrium constants for reaction and sorption (K_r and K_a) can all be expressed in the standard Arrhenius form:

$$k = k_\infty e^{-E/RT} \qquad (15)$$

$$K = K_\infty e^{-\Delta H/RT} \qquad (16)$$

where T is the absolute temperature, k_∞ is the rate constant at very high temperature (Arrhenius frequency factor), E is the chemical activation energy (J/mol), R is the ideal gas law constant (J/mol·K), K_∞ is the value of the equilibrium constant at very high temperature, and ΔH is the energy of reaction or sorption (J/mol).

As the temperature increases, equation (15) predicts that the rate constants will also increase. For endothermic reaction or sorption, equation (16) predicts that as the temperature increases the equilibrium constant will also increase, while for exothermic processes, higher temperatures will result in a lower equilibrium constant. It can be shown from kinetic theory that the difference between the activation energies of the reverse and forward processes ($E_1 - E_2$) is approximately equal to the energy of reaction or sorption [11]. If the temperature remains constant during the time taken for chemical species to pass into the concrete, all the kinetic and thermodynamic constants will themselves be constant. For liquid systems normal pressure levels have little or no effect on sorption and reaction rate law model constants.

3.5 Conservation Balances

The overall conservation equations governing the rate at which chemical species penetrate concrete will depend on the rate laws for the processes which are occurring within it. The system on which the conservation balances are made is the pore solution contained within a thin element of width dz and cross section S located within the slab (refer to Fig. 3). Transport is presumed to only occur through the slab in the z direction.

An overall conservation balance for each penetrant within the system takes the form:

Rate of Accumulation = Net Rate of Diffusion + Net Rate of Convection - Rate of Disappearance by Sorption - Rate of Disappearance by Reaction. (17)

Equation (17) represents a molar inventory for each species. The units on each term are moles per unit time. The net rate refers to the rate of input to the system minus the rate of output.

3.5.1 Dimensional Form

Application of rate laws for diffusion and convection (equations (5) and (7)) to equation (17) leads to:

$$\frac{\partial C_A}{\partial t} = \frac{D_{eA}}{\epsilon} \frac{\partial^2 C_A}{\partial z^2} - v \frac{\partial C_A}{\partial z} - \frac{S_g}{V_g} (-r_A) \qquad (18)^+$$

where S_g is the surface area of the pores (m^2/kg) and V_g is the pore volume (m^3/kg). Both S_g and V_g are based on the mass of cement or concrete. They are presumed constant in this formulation.

Pore surface area, pore volume and porosity are all physical parameters of the pore structure which can be measured independent of transport processes. The term $-r_A$ represents the rate of sorption or reaction per unit area of pores. Equation (18) is a second order partial differential equation whose solution gives $C_A(z,t)$, the concentration of penetrant as a function of depth into the slab z and exposure time t. The equation will be linear if the sorption or reaction rate ($-r_A$) is itself linear.

$^+$The ratio of S_g to V_g can also be written as $(S/V)_g$.

3.5.2 Dimensionless Form

Equation (18) can be given in the following dimensionless form:

$$\frac{\partial C}{\partial t'} = \frac{\partial^2 C}{\partial x^2} - Pe \frac{\partial C}{\partial x} - r_d \qquad (19)$$

with dimensionless concentration $C = C_A/C_{AO}$, dimensionless time $t' = D_{eA}\, t/\epsilon L^2$, dimensionless distance $x = z/L$ and dimensionless reaction rate r_d given by:

$$r_d = \frac{S_g}{V_g} \frac{\epsilon L^2}{D_{eA}\, C_{AO}} (-r_A) \qquad (20)$$

Both the Peclet number Pe and time ratio t' of Table 2 appear in this analysis.

3.5.3 Initial and Boundary Conditions

Equations (18) or (19) can be solved if one initial and two boundary conditions are provided. The initial condition gives the initial concentration profile of species A within the pores of the slab. It can be written as $C = C_0(x)$, where C_o is the dimensionless initial concentration C_{OA}/C_{AO}. Although, in general, the initial condition will be a function of position, a special case of interest occurs when

this concentration is initially constant or zero. $C_{OA}=0$ occurs when there is initially no A within the cement pores.

The boundary conditions describe how the concentrations change with time at the ends of the slab. There are three types of common boundary conditions: (1) imposed, (2) zero flux, and (3) Danckwert [12]. Table 5 summarizes these types. Both dimensional (z,t) and dimensionless (x,t') conditions are given. Two boundary conditions of one or more type need to be specified, one at each end of the slab. Imposed conditions impress the concentration of the external solution on the ends of the slab. These conditions can change with time as, for example, when reservoirs of finite size are present at the ends of the concrete slab, or when the external environment changes. The zero flux conditions, shown in the second column of Table 5, will apply when the ends of the slab are impermeable, as would be the case when an inside liner is used.

The Danckwert conditions [12] given in the last column of table 5 can apply when there is convection in the positive z direction. In the Danckwert formulation the external solutions on both sides of the slab are considered to be well mixed. The conditions represent species inventories at the slab ends. There is an abrupt drop in the concentration of A (at z=0) when passing in the flow direction from the

Table 5. Types of Boundary Conditions

Location[a]	Imposed	Zero Flux	Danckwert[b] [12]
$z = 0$	$C_A = C_{Ain}(t)$	$\frac{\partial C_A}{\partial z} = 0$	$\epsilon v C_{Ain} = \epsilon v C_{AO} - D_{eA} \frac{\partial C_A}{\partial z}$
$x = 0$	$C = C_{in}(t')$	$\frac{\partial C}{\partial x} = 0$	$C_{in} = C_o - \frac{1}{Pe} \frac{\partial C}{\partial x}$
$z = L$	$C_A = C_{AL}(t)$	$\frac{\partial C_A}{\partial z} = 0$	$\frac{\partial C_A}{\partial z} = 0$
$x = 1$	$C = C_L(t')$	$\frac{\partial C}{\partial x} = 0$	$\frac{\partial C}{\partial x} = 0$

[a] z conditions apply to equation (18), x conditions to equation (19).

[b] conditions are for flow in the positive z direction; for flow in the opposite direction the conditions in this column are reversed (see text).

external solution to the inside of the slab. Thus C_{Ain}, the concentration in the upstream reservoir, will be greater than C_{AO}, the concentration at the slab entrance. At high values of the Peclet number, corresponding to high flow rates, and low diffusivities and thick slabs, the Danckwert condition at the upstream end reduces to the imposed condition $C_{Ain} = C_{AO}$. A zero flux condition arises at z=L, even with convection, because the concentration of the solution exiting from the pores of the slab (C_{AL}) will be the same as the concentration in the external solution (C_{Aout}). When flow is in the opposite direction the boundary conditions must be reversed, with a zero flux condition at z=0, and the condition containing the Peclet number at z=L.

3.5.4 Molar Flow and Retention of Chemical Species

The service life of concrete exposed to deleterious aqueous solutions of salts and dissolved gases largely depends on their concentrations within the concrete pores. Therefore, it is important to know the amount of deleterious chemical species which has passed into or through concrete members in a given time.

In the absence of flow, the total moles of chemical A, M_{AO}, which has passed into the concrete in time t will be given by:

$$M_{AO} = S \int_0^t N_A|_{z=0}\, dt \tag{21}$$

When convection is also present, the total flow of deleterious chemical species into and through the slab must also include the convective flow in addition to the diffusive flow. Under this condition the total moles of chemical A which has passed into the slab by time t is:

$$M_{AO} = \int_0^t (SN_A + F_A)|_{z=0}\, dt = Q\, C_{Ain}\, t \tag{22}$$

The second equality in equation (22) follows directly from the Danckwert condition at z=0. The total amount which has passed completely through the slab is:

$$M_{AL} = \int_0^t F_A|_{z=L}\, dt = Q \int_0^t C_{AL}\, dt \tag{23}$$

In equation (23) the Danckwert boundary condition has been used ($\partial C_A/\partial z = 0$ at $z = L$) where C_A is given by the solution to equation (18). If flow were reversed, N_A would appear in equation (23) rather than (22). The difference between M_{AO}

slab at time t in addition to the amount which has adsorbed or reacted up to that time. At steady state the diffusive flux of A, N_A, will be a constant and the transport of A out of the slab will be reduced by the amount of reaction or sorption which occurs.

When dissolved A reacts with one or more of the solid concrete constituents, the process could require many years to reach a true steady state. Often, however, it is reasonable to assume a pseudo-steady state (also referred to as quasi-steady state) where the reaction or sorption proceeds much slower than the time taken for the concentration profiles to re-establish themselves as a result of these processes. This is especially the case for moving interface problems, where, e.g., a reaction front slowly moves through the slab as chemical A reacts with a concrete constituent. Mathematically, quasi-steady state implies that over any finite time interval, the molar accumulation term $\partial C_A/\partial t$ is equal to zero in the conservation balances. In Sections 4.2 and 4.3, models are developed and applied for cementitious systems which can be characterized by quasi-steady state processes.

4. APPLICATION OF MATHEMATICAL MODELS

A general mathematical model was formulated in Section 3 which incorporates the important processes controlling the rates and amount of deleterious species transported into concrete buried underground. In this section, mathematical solutions are developed for the general model as well as sub-models for specific applications. Separate models are developed and solved for chloride ion penetration of concrete, for leaching of concrete constituents, and for sulfate attack of concrete. These solutions can be applied to the prediction of the concentration and transport rates of chloride ions, sulfate ions and dissolved carbon dioxide species through concrete.

4.1 Chloride Ion Penetration

Chloride ions can be transported into concrete by diffusion and convection. The penetration of chloride ion is undesirable since it is known to accelerate the corrosion of steel reinforcing bars in concrete [13]. When water and oxygen are also present, the chloride ion may depassivate steel and thus directly raise the rate of the anodic half cell reaction given by:

$$Fe \rightarrow Fe^{++} + 2e^{-} \qquad (24)$$

Chloride ions can also catalyze the transfer of charge. In both cases the rate of corrosion is higher with increased ion concentration. The threshold concentration at which chloride initiates corrosion decreases as the pH is reduced [13]. Thus, the presence of dissolved carbon dioxide along with chloride ion can significantly accelerate corrosion of reinforcing steel. Since chloride ions do not appear to be consumed in this process, concentrations will rise at the steel surface and further accelerate corrosion.

4.1.1 Absorption and Reaction of Chloride Ions

Reaction of chloride ions with calcium aluminates can produce chloroaluminates. Also, chloride ions can be adsorbed on the pore walls, slowing the transport process of chloride ions and lowering the accumulation of chloride ions in the pore solution. Tuutti [14] presents a model in which the reaction and adsorption of chloride ions results in an apparent diffusion coefficient D_a which is less than the effective value D_e by the factor g. Thus:

$$D_a = g\, D_e \tag{25}$$

where g is the ratio of the concentration of chloride ions in solution to the total concentration, i.e., those in solution plus those reacted and adsorbed on the surface of

pores. If none of the chloride ions are removed from solution g = 1, while g = 0 indicates that all of the chloride ions have been removed from solution. Other authors have used a similar formulation [15,16].

Tuutti's model takes the form:

$$\frac{\partial C_A}{\partial t} = D_a \frac{\partial^2 C_A}{\partial z^2} \tag{26}$$

with D_a given by equation (25).

Analysis of this model shows that it does not account for all surface phenomena. As discussed in Section 3, diffusion coefficients for ions depend on pore structure, the size and charge of the diffusing ions, and temperature, but not on the amount adsorbed or reacted. Further, small values of the factor g could indicate that pore concentrations have not reached steady state. A more complete formulation incorporates surface phenomena as a sink term, as is presented in the last term of equation (18).

4.1.2 Model Simplifications

With first order reaction or adsorption, equations (18) and (19), become, respectively, equations (27) and (28):

$$\frac{\partial C_A}{\partial t} = \frac{D_{eA}}{\epsilon} \frac{\partial^2 C_A}{\partial z^2} - v \frac{\partial C_A}{\partial z} - k\,(S/V)_g\, C_A \qquad (27)$$

$$\frac{\partial C}{\partial t'} = \frac{\partial^2 C}{\partial x^2} - (Pe) \frac{\partial C}{\partial x} - m^2\, C \qquad (28)$$

In equation (27), k is either the adsorption constant k_a or the first order reaction rate constant k_1. Equation (28) has the two dimensionless parameters, the Peclet number; and the modulus m given by:

$$m = \left[\frac{\epsilon k}{D_{eA}} (S/V)_g\, L^2\right]^{1/2} \qquad (29)$$

m^2 represents the maximum value of the first order dimensionless reaction rate r_d. It is equal to the value of r_d at concentration C_{AO}, and it is referred to as the Damkohler number [17]. In chemical reactor theory m, itself, is known as the Thiele modulus (refer to Table 1). It is a dimensionless reaction-diffusion constant which measures the relative importance of diffusion and reaction (or sorption). The significance of the magnitude of the

Thiele modulus to service life prediction of concrete exposed to chloride ion is discussed at the end of this section.

With no convection, equations (27) and (28) reduce, respectively, to equations (30) and (31):

$$\frac{\partial C_A}{\partial t} = \frac{D_{eA}}{\epsilon} \frac{\partial^2 C_A}{\partial z^2} - k\,(S/V)_g\, C_A \qquad (30)$$

$$\frac{\partial C}{\partial t'} = \frac{\partial^2 C}{\partial x^2} - m^2\, C \qquad (31)$$

Note that equation (30) has a different functional form than equation (26). This shows that it is an approximation to base the formulation only on an attenuation of the diffusion coefficient. Because of the large number of possible boundary and initial conditions to which these equations can be subject (refer to Table 5) it is not possible to present all of the solutions for each possible physical situation. Rather, one particular realistic case will be solved and discussed.

This case is shown schematically in Figure 4, where a concrete member is subjected to a constant environment of chloride ion of concentration C_{Ain} at one end ($z = 0$), while at the far end ($z = L$) a protective liner presents an

impermeable barrier. (The case where a free surface exists, as in an underground concrete vault, can be solved also by the following methods.) Thus, there is an imposed boundary condition at z = 0 and a zero flux condition at z = L. The concrete is presumed to be initially saturated with pore water which is chloride free, so that $C_{OA} = 0$, while the steel reinforcing bar is vertically embedded somewhere within the concrete matrix (shown dashed in Figure 4). Its presence does not influence transport processes. In the present case, there is no convection, and diffusion occurs only in the z direction. The analytical relationships to predict the concentration profile $C_A(z,t)$ [or $C(x, t')$] of chloride ion within the concrete member need to be developed. Because of symmetry this problem is equivalent of one where no liner is used and concentration C_{Ain} is imposed simultaneously on both ends of a specimen of length 2L. In both problems z = L is a vertical plane of zero flux.

Solutions to equation (31) can be obtained by using several different methods. These include analytical methods such as Laplace transforms, separation of variable techniques, and numerical methods. Analytical solutions are preferred since they show the precise effect of system variables and dimensionless groups. However, analytical solutions are generally possible only when the equations of the model are

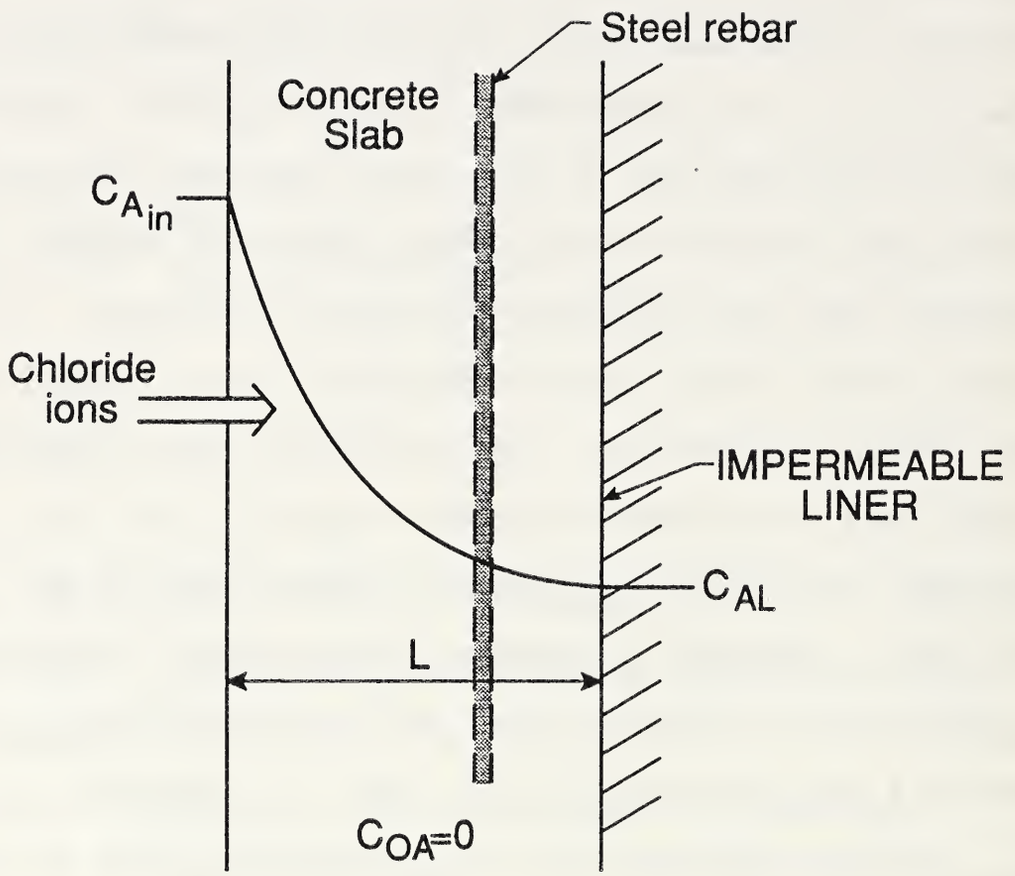

Figure 4. Model system for chloride ion diffusion through concrete.

linear, as is true in the present case. Analytical methods produce solutions expressed as infinite series of terms, each of which is a function of time and position. The separation of variables method gives solutions which converge most rapidly at long dimensionless times t', so that fewer terms in the resulting series are needed. Laplace transform methods, on the other hand, yield solutions which converge most rapidly at shorter times.

4.1.3 Solutions to Models

For the problem considered, dimensionless concentration profiles of chloride ion C(x, t') were obtained for both large and small dimensionless times. Also, expressions for dimensionless concentrations at the liner surface (z = L or x = 1) were found. Steady state ($\partial C_A/\partial t = 0$) mathematical solutions for chloride concentration and solutions in which reaction is not significant were also derived.

Table 6 gives the short time solutions [equations (32) to (35)] obtained by the method of Laplace transforms while Table 7 gives the long time model solutions [equations (36) to (39)] obtained by the method of separation of variables.

In addition to the concentration-time profiles (C,t') solutions are presented in Tables 6 and 7 for dimensionless

concentrations at the liner surface (x=1) and for the sub-case when there is no reaction or adsorption (m=0). Both the short and long time model solutions are expressed in terms of an infinite series of trigonometric and exponential functions.

At small values of the dimensionless time (t'), when there is little or no reaction or adsorption, equation (32) applies. At still smaller values of t' the infinite series in this equation can be shown to reduce to:

$$C_A = C_{Ain} \operatorname{erfc}\left[\frac{\epsilon z^2}{4 D_{eA} t}\right]^{1/2} \qquad (40)$$

This solution agrees with the result which is obtained when the slab is treated as being semi-infinite [2]. It is also similar to the equations given by Atkinson [18] and Lawrence [19].

The concentrations at the liner or free surface depend on t' and the degree to which the concrete is effective in removing chloride. Permeation to the surface becomes important at times t when the dimensionless time (t') is of the order of unity. As discussed in Section 2 of this report, the value of t' controls the rate at which steady-state is attained rather than the absolute time t. For

Table 6. Short Time Model Solutions

Concentration-Time Profiles

$$C = \frac{1}{\sqrt{4\pi}} \sum_{n=0}^{\infty} (-1)^n \{(2 + 2n - x) \int_0^{t'} \frac{\exp - [\frac{(2+2n-x)^2}{4u} + m^2 u]}{u^{3/2}}$$

$$+ (2n + x) \int_0^{t'} \frac{\exp - [\frac{(2n+x)^2}{4u} + m^2 u]}{u^{3/2}} \} \qquad (32)$$

Reaction/Adsorption Insignificant (m=0)

$$C = \frac{1}{\sqrt{4\pi}} \sum_{n=0}^{\infty} (-1)^n \{(2 + 2n - x) \int_0^{t'} \frac{\exp - [\frac{(2+2n-x)^2}{4u}] \, du}{u^{3/2}}$$

$$+ (2n + x) \int_0^{t'} \frac{\exp - [\frac{(2n+x)^2}{4u}] \, du}{u^{3/2}} \} \qquad (33)$$

Concentration-History at Concrete-Liner Interface (x=1)

$$C = \sum_{n=o}^{\infty} (-1)^n [e^{(2n+1)m} \operatorname{erfc} (\frac{2n+1}{2\sqrt{t'}} + m\sqrt{t'} \qquad (34)$$

$$+ e^{-(2n+1)m} \operatorname{erfc} (\frac{2n+1}{2\sqrt{t'}} - m\sqrt{t'})]$$

Reaction/Adsorption Insignificant (m=0)

$$C = 2 \sum_{n=o}^{\infty} (-1)^n \operatorname{erfc} (\frac{2n+1}{2\sqrt{t'}} \qquad (35)$$

Table 7. Long Time Model Solutions

Concentration-Time Profiles

$$C = \frac{\cosh m(1-x)}{\cosh m}$$

$$- \pi \sum_{n=1}^{\infty} \frac{(-1)^{n+1}(2n-1)\cos\left[(2n-1)\frac{\pi}{2}(1-x)\right] \exp - \left[m^2 + (2n-1)^2 \frac{\pi^2}{4}\right]t'}{m^2 + (2n-1)^2 \frac{\pi^2}{4}} \quad (36)$$

Reaction/Adsorption Insignificant (m=0)

$$C = 1 - \frac{4}{\pi} \sum_{n=1}^{\infty} \frac{(-1)^{n+1}}{(2n-1)} \exp\left[-(2n-1)^2 \frac{\pi^2}{4} t'\right] \cos\left[(2n-1)\frac{\pi}{2}(1-x)\right] \quad (37)$$

Concentration-History at Concrete-Liner Interface (x=1)

$$C(1) = \operatorname{sech} m - \pi \sum_{n=1}^{\infty} \frac{(-1)^{n+1}(2n-1) \exp - \left[m^2 + (2n-1)^2 \frac{\pi^2}{4}\right] t'}{m^2 + (2n-1)^2 \frac{\pi^2}{4}} \quad (38)$$

Reaction/Adsorption Insignificant (m=0)

$$C(1) = 1 - \frac{4}{\pi} \sum_{n=1}^{\infty} \frac{(-1)^n}{2n-1} \exp\left[\frac{-(2n-1)^2\pi^2}{4}\right] t' \quad (39)$$

$t' > 1$ the long time model solutions of Table 7 should be used. For dimensionless times near unity either set of solutions produce equivalent answers, with a similar number of terms needed for convergence in the infinite series. At such times, the chloride or other penetrant concentrations at the surface adjacent to the liner or free surface will have risen to within a significant fraction of their final or steady-state values. For $t' < 1$ the short time model solutions of Table 6 should be used.

4.1.4 Corrosion of Reinforcing Steel Embedded in Concrete

These analyses demonstrate that the durability of reinforced concrete exposed to corrosive amounts of chloride ions will be enhanced if D_e is small, L is large and ϵ is small. The most sensitive of these parameters is the slab thickness, L. For a concrete slab twice as thick, it takes four times as long for the chloride to reach a given fraction of its final concentration. Therefore, to increase the service life of reinforced concrete by preventing the accumulation of a threshold concentration of chloride ions at the steel surface, it is recommended to have a thick concrete cover member over the reinforcing bars, made of dense concrete (low ϵ and D_e). Although these results are qualitative, the actual model solutions can give a precise prediction of the effects of these variables.

Concentrations of intruding chloride ions in concrete also depend on the affinity of the chloride for cement paste. A quantitative measure of this effect is provided by the Thiele modulus m as defined by equation (29). As discussed in Section 2, the Thiele modulus measures the relative importance of diffusion to reaction. High values correspond to diffusion control while low values correspond to reaction or adsorption control. It has been shown that diffusion control occurs when $m > 5$ while reaction control occurs when $m < 0.2$ [11].

As shown by equation (29), the modulus m is a function of the surface-to-volume ratio $(S/V)_g$, the slab thickness L, the effective diffusivity D_{eA}, and the affinity of the cement paste for the chloride ion, as measured by the reaction or adsorption constant k. Depending on the cement used and the temperature, m can take on any positive value. The greater the retention of chloride within the cement by reaction or adsorption with tricalcium aluminate or other constituents, (high k), the higher will be the modulus, and the more likely diffusion will control. The value of m will be small if the cement only contains small amounts of aluminate or other constituents which can react with chloride ions. If the tricalcium aluminate is the major reactive constituent and it has already reacted to form ettringite or monosulfate, then m will again be small. In

these cases k will be low and transport will only occur by diffusion.

Even in the worst possible case, where k = 0, and there is no protection by reaction or adsorption with cement constituents, it is still possible to have low concentrations at the steel surfaces since these concentrations do not reach an appreciable fraction of their final steady-state values until the dimensionless contact time t' is approximately unity. A sample calculation illustrating this effect was previously presented (Section 1.2). It follows from equation (36) that the steady state concentration of chloride ions at the surface of a rebar embedded midway in a concrete slab of thickness 2L, when both sides of the slab are simultaneously exposed to an external concentration C_{Ain}, is given by:

$$C_A = C_{Ain} \text{ sech } m \qquad (41)$$

At low values of the parameter m, the concentration of chloride ion at the rebar surface will eventually reach the concentration in the outside solution C_{Ain}. Whether or not corrosion will occur at the rebar surface will depend on the temperature, concentration of dissolved oxygen, pH, and the electrochemical potentials of the half-cell reactions. In some instances corrosion will not initiate regardless of the oxygen concentration at the corrosion site because it is

thermodynamically unfavorable, e.g., when a stable passive oxide film is formed. However, chloride ion can catalyze the breakdown of this film. Further experimental and theoretical studies need to be directed towards determining and predicting both the rate of penetration of oxygen through concrete and the catalytic effect of chloride ion on corrosion rates. Also, for predicting the corrosion of concrete structures buried underground, the concentration of oxygen as a function of soil depth needs to be known. The models presented here can help by providing a prediction of the amount of chloride ion which is present at the potential corrosion site within the reinforced concrete. They can also be used to predict concentration profiles of oxygen.

4.2 Leaching of Concrete Constituents

Hardened cement paste contains constituents which can be removed by leaching when subjected to attack by acidic or neutral groundwater. These include dissolved alkali oxides, K_2O and Na_2O (saturated solution pH $\approx$ 13.5), $Ca(OH)_2$ (saturated solution pH $\approx$ 12.5) and calcium silicate hydrate gel, CSH (saturated solution pH $\approx$ 10.5) [20]. The acidic groundwater is present in the form of dissolved carbon dioxide gas (CO_2), carbonic acid (H_2CO_3) or bicarbonate ion (HCO_3^-).

Leaching by acidic groundwater (acid leaching) occurs more rapidly than leaching by neutral groundwater (water leaching). When transport is diffusion controlled the concentration of acidic species at the reaction interface will be lower, thereby raising transport rates. With water leaching, the diffusion of the basic species back out through the concrete controls transport. Since solubilities are relatively low, the basic species will leach from the concrete more slowly. When transport is reaction controlled, acid leaching raises reaction rates since acid concentrations will be high at the reaction front. This is in contrast to water leaching where no reaction occurs. Discussion in this and subsequent sections is restricted to acid leaching. Groundwater leaching is considered in Section 4.3.3.1, where mathematical models are developed for the leaching of gypsum.

Acidic groundwater will successively leach out each of the basic cement constituents beginning with the alkali oxides, which are the most basic and most soluble constituents, and ending with the calcium silicate hydrate (CSH) gel. Over many years the pH of the pore solution can decrease until it is in equilibrium with either CSH gel or the external groundwater [20]. By leaching the alkaline cement constituents, especially calcium hydroxide, the porosity of the cement matrix increases. This can drastically lower strengths and facilitate ingress of other deleterious

chemical species such as sulfate and chloride ions. The deleterious effects are compounded when steel rebars are used since lower pH and higher concentrations of chloride ion act together to accelerate corrosion.

4.2.1 Alkali Oxides and Hydroxide

The alkali oxides are present in relatively small amounts and are generally found near the surface of the individual cement particles where they can readily dissolve. The leaching of these compounds should occur relatively rapidly when the outside of the hardened cement paste (HCP) is exposed to acidic, neutral or even alkaline groundwater. For neutral (pH ≈ 7) or acidic groundwater, the leaching mechanism is most likely to be diffusion controlled since acidic groundwater can rapidly react with alkali hydroxide. For example, carbonic acid can react with potassium oxide within the HCP to form dissolved potassium carbonate and water:

$$H_2CO_3 + 2\ KOH \rightarrow K_2CO_3 + 2\ H_2O \qquad (42)$$

If the supply of groundwater is sufficient, the acid in the groundwater can completely neutralize the alkali hydroxides. Such neutralization reactions may proceed as a wave or moving front through the concrete, with acid-laden groundwater on one side and saturated KOH or NaOH solution on the other. The leaching of alkali from cement paste will

be complicated by the hydration reactions which may occur at the same time. Removal of hydroxide ions by leaching of alkalies can stimulate cement hydration by promoting crystallization of additional calcium hydroxide crystals. A more complete analysis, which is beyond the scope of the report, would involve ion inventories for each ion present in the pore solution of the cement paste [21].

4.2.2 Calcium Hydroxide

The principal alkaline constituent of HCP is calcium hydroxide which can comprise 20-25% by volume of the cement matrix. Calcium hydroxide grows away from the cement grains into the capillary space between cement particles as relatively large hexagonal prisms [19]. These $Ca(OH)_2$ crystals will continue to grow as long as cement hydration occurs. Their removal by acid attack may promote additional hydration both by providing a sink for hydroxide ion and by exposing fresh surface to the pore water. The models developed in the next section presume that hydration is essentially complete before significant acid attack begins.

Calcium hydroxide is both less soluble and less accessible than the alkali oxides. Thus, it is removed by leaching after the alkalies. Most of the neutralization capacity of the HCP is contained within the calcium hydroxide. Thus, models for its consumption by acidic groundwater attack are

more important than those for the leaching of alkalies. Nevertheless, knowledge of the mechanism rates of alkali removal is important because its neutralization capacity provides a factor of safety.

Leaching mechanisms for calcium hydroxide involve its attack by carbonic acid and bicarbonate ions. Dissolved carbon dioxide or carbonic acid neutralizes calcium hydroxide directly:

$$H_2CO_3 + Ca(OH)_2 \rightarrow CaCO_3 + 2\ H_2O \qquad (43)$$

Groundwaters containing carbonic acid can be partially neutralized by calcareous aggregate forming the bicarbonate [22] ion, which can react further with additional calcium hydroxide:

$$Ca(HCO_3)_2 + Ca(OH)_2 \rightarrow 2CaCO_3 + 2\ H_2O \qquad (44)$$

Solutions of calcium carbonate in water have a slightly alkaline pH. Precipitated calcium carbonate has nearly the same density as that of the calcium hydroxide it replaces. Thus volume changes are not as important in carbonate leaching processes as in other deleterious processes such as sulfate attack. The calcium carbonate product will precipitate when the Langelier (or saturation) index [23] is positive. The Langelier index is a function of pH, total

alkalinity and solids, and calcium content of the water. It is a measure of potential leaching capability of acidic groundwaters. When the index is negative the water is low in lime (soft), and it can dissolve calcium from hardened cement paste.

4.2.3 Calcium Silicate Hydrate

When nearly all the calcium hydroxide has been neutralized, the calcium silicate hydrate or cement gel (CSH) will start to be removed from the concrete matrix. The bicarbonate ion can react with the calcium of the CSH. Water containing more than 20 ppm of dissolved carbon dioxide can result in the deterioration of hydrated cement paste [24]. As the lime to silica ratio (C/S) in the gel decreases, the pH falls. When the ratio reaches 0.85 the cement gel begins to dissolve congruently at a pH of around 10.5. After the CSH has been totally dissolved the pH will reach that of the pore solution. This pH lies somewhere between that of the outside acidic groundwater and that created by the residue salts in the original concrete [20, 22]. CSH removal occurs on time scales much longer than the dissolution of calcium hydroxide. The leaching of CSH should occur only over centuries and should not be of concern in predicting the service life of underground concrete vaults for disposing of LLW. For this reason, mathematical models for its removal will not be developed in this report.

4.2.4 Mathematical Models for Leaching of Concrete Constituents

The mathematical models developed here are based on the same model system as considered in Section 3.1 and depicted in Figure 3. Transport is considered to occur in only the z direction as a result of the mechanisms of diffusion, convection, dissolution, reaction and adsorption. The transported model species A can be either dissolved alkali oxides, carbon dioxide, carbonic acid or bicarbonate ion. As discussed in the last section, these have similar neutralizing reactions and much of the theory presented can be used interchangeably for these species.

From a generic point of view all of the neutralization reactions can be written:

$$A + B \rightarrow AB + H_2O \qquad (45)$$

where A represents the acidic component, B the basic component with which it reacts and AB the neutralization product, which may or may not be soluble.

4.2.4.1 Leaching of Alkali Oxides

Based on equations (42) and (45), A represents carbonic acid, B represents potassium hydroxide and AB is potassium carbonate. Since the alkali carbonates are soluble they will be able to diffuse out of the pores. Very little additional porosity is created on dissolution because of the small volume fraction of the alkali oxides. In the conceptual model, it is presumed that the pores of HCP are initially saturated with KOH at concentration C_B^* and that the outside of the slab is subjected to acidic groundwater of concentration C_{AO}. The transport mechanisms are considered to be dissolution, reaction and diffusion. The reaction is presumed to be first order in each reactant so that:

$$-r_A = k\, C_A\, C_B = k\, C_A\, C_B^* = k'\, C_A \qquad (46)$$

Until completely dissolved, the solid KOH will maintain a local saturation by further dissolution, so that $C_B = C_B^*$, as shown in equation (46). The reaction then becomes pseudo-first order with modified rate constant k' equal to kC_B^*. In this case, equations (29) and (30) apply with the k of equation (29) replaced by k' in the definition of the Thiele modulus m. Thus, the equations in Tables 6 and 7 will govern the acid concentration profile within a slab whose near side is exposed to solution of concentration C_{Ain}

and whose far side is made impermeable using a liner or concrete coating. Alternatively, they will predict the concentrations in a slab of thickness 2L when both sides are simultaneously exposed to solution of concentration C_{Ain}.

The discussion in Section 4.1.3 is also applicable to the present situation. The depth of penetration of acid attack will depend on both the dimensionless time and the reaction-diffusion modulus. The rate of diffusion of acid should be similar to that of chloride ions since the cement pore structure is the same and the magnitude of the free stream or molecular diffusion coefficients for chloride and carbonate or bicarbonate ions are similar [25]. Thus the value of t', the reduced time, will be nearly the same for both systems. The value of the Thiele modulus m should be higher for transport of acid into concrete than for chloride ion because acid-base reactions are both inherently faster and occur in more places than the reaction of chloride ions with hydrated tricalcium aluminate. The reaction of alkali hydroxide with carbonic acid will be more of a volume phenomenon than a surface area one. When the carbonic acid reacts with calcium hydroxide the modulus m will similarly be high because the neutralization reaction is quite rapid, and because the calcium hydroxide occupies a large exposed portion of the surface area available to the pore solution. When m is high, transport of carbonic acid into the concrete will become diffusion controlled, and it is likely that a

interface or front will move through the concrete. The model solutions show that when the modulus m is higher at the same effective diffusivity D_{eA}, that the relative concentrations of C_A and C_{Ain} will decrease much faster and reach lower final values than when m is lower. Thus, it will take longer for the intrusion of acid than for the intrusion of chloride ion.

Since the principal neutralization potential of the concrete is provided by the calcium hydroxide, and since the neutralization mechanisms are similar to both these for alkali oxide and calcium hydroxide, the mathematical models and solutions are deferred to the next sub-section.

4.2.4.2 Leaching of Calcium Hydroxide

Most of the discussion on the acid leaching of alkali hydroxides is applicable to the acid attack of calcium hydroxide. The principal difference involves the differences in the solubilities of the reaction products: calcium carbonate is relatively insoluble, calcium hydroxide has limited solubility, while the respective alkali salts have appreciable solubilities. In this section the leaching processes of calcium hydroxide is presumed to follow equations (43) and (45). Reactant A is carbonic acid, reactant B is solid calcium hydroxide, and product AB is precipitated calcium carbonate.

Figure 5 shows the model system for the leaching of calcium hydroxide from concrete. In the conceptual model development the pores of the HCP in the concrete slab are taken to be saturated with calcium hydroxide solution at concentration C_B^* in equilibrium with the solid. At the time when the calcium hydroxide leaching begins (t_o) the alkali oxides and their products are considered to have been leached from the concrete. The amount of calcium hydroxide which may have been neutralized along with the alkali oxides before time t_o is neglected. At time t_o the slab is subjected to an external acid solution of concentration C_{Ain}. It is assumed that circulation keeps this solution well mixed, so that there are no outside diffusional resistances.

Since the use of a liner or facing on the inside of the concrete slab will help prevent flow, in this development the effects of internal convection or flow are presumed to be negligible. The effect of convection on the transport process is considered in the next section where models for sulfate attack are developed. The model given there can be easily modified to account for convection in the present case.

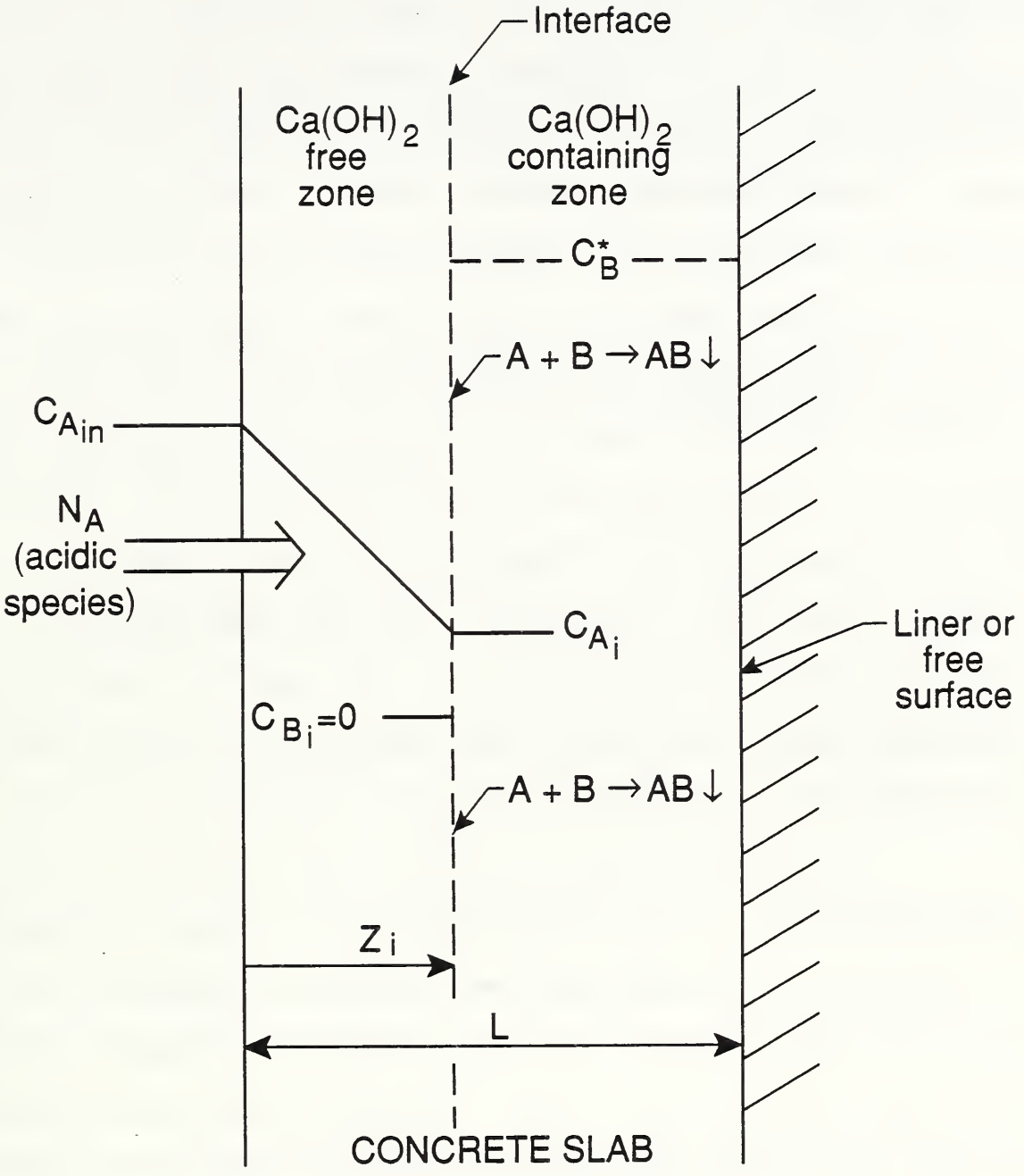

Figure 5. Model system for leaching of calcium hydroxide from concrete.

Consider acid attack of calcium hydroxide for the case where the reaction-diffusion modulus m is low. A point will be reached where the local calcium hydroxide near the outside of the slab (z=0) is completely consumed by the penetrating acid solution. A moving interface might then move into the slab. However because reaction rates are small compared to diffusion rates the acid concentration at the interface would be greater than zero since some acid would have been able to diffuse past the current interface. With time, the interface would move through the slab but at a faster rate than for a totally diffusion controlled situation (high m). The acid concentration within the slab would gradually rise towards its surface value C_{AO}. When the interface had completely moved through the slab, the calcium hydroxide originally contained within the concrete would have been neutralized by the carbonic acid.

In the limit of a very large modulus m, a reaction front or interface will move through the concrete as depicted in Figure 5. Because the reaction is diffusion controlled it will only occur at this front. Because the neutralization reaction is rapid, the concentrations of A and B will be low at the interface. In the limit of very rapid reaction it will approach zero. The concentration gradient of A will be linear from the surface (z=0) to the interface ($z=z_i$), while that of B will drop abruptly from C_B^* to its concentration corresponding to the dissociation equilibrium of AB. At the

interface the stoichiometry of the reaction requires that the molar consumption rate of A be equal to that of B. The interface gradually moves through the concrete, but at a slower and slower rate as time proceeds, since the acid must continuously travel a longer distance to arrive at the reaction front.

We can express this scenario mathematically by equating the flux of acid (A) into the slab to the consumption of base (B) at the reaction interface:

$$N_A = - D_{eA} \left(\frac{\partial C_A}{\partial z}\right)_{z=0} = - D_{eA} \left(\frac{\partial C_A}{\partial z}\right)_{z=zi} = \rho_B f_B \frac{dz_i}{dt} \qquad (47)$$

where ρ_B is the molar density of the solid calcium hydroxide and f_B is its volume fraction in the concrete. It is implicitly assumed that all the calcium hydroxide is accessible to acid attack through the pores. The value of f_B can be determined based on a knowledge of the initial concrete composition and the degree of cement hydration.

In equation (47) the flux of A at z=0 has been taken equal to that at $z=z_i$, which assumes quasi-steady state (QSS), so that the accumulation term $\partial C_A/\partial t$ is small. This implies that once an initial steady state is reached, there is little change in solution concentration as the interface retreats and the system continually adjusts to each new

steady state. The QSS assumption has been shown to be accurate for solid-liquid systems which involve the dissolution of soluble salts [26]. It is even more likely to be valid for salts of low to moderate solubility. Invoking the QSS assumption, equation (47) becomes:

$$\rho_B f_B \frac{dz_i}{dt} = D_{eA} \left(\frac{C_{AO} - C_{Ai}}{z_i}\right) = k' C_{Ai} \qquad (48)$$

As given by equation (48) the diffusive flux of A at the moving interface (N_{Ai}) has been taken equal to the rate at which A reacts there, i.e., ($-r_{Ai}$). The rate of interface movement varies inversely with f_B, the volume fraction of calcium hydroxide in the pores. This is consistent with the prediction that the reaction interface will move inwards more rapidly when there is less calcium hydroxide to neutralize. Solving the last equality in equation (48) for C_{Ai}, the interfacial acid concentration:

$$C_{Ai} = \frac{C_{AO}}{1 + k' z_i / D_{eA}} \qquad (49)$$

Substituting equation (49) into (48), separating variables and integrating, with z_i=0 at t=0:

$$z_i + \frac{k'}{2D_{eA}} z_i^2 = \frac{k' C_{AO}}{\rho_B f_B} t \qquad (50)$$

This relation predicts the way the interface will move through the concrete slab as a function of time. The total time θ_L taken for the interface to pass completely through the slab is given by:

$$\theta_L = \frac{f_B \rho_B L}{k' C_{AO}} \left(1 + \frac{k' L}{2\ De_A}\right) = \frac{\rho_B f_B L^2}{C_{AO} D_{eA} Da} \quad (1 + 1/2\ Da) \qquad (51)$$

Equations (50) and (51) can also be compactly written in dimensionless form as, equation (52) and (53), respectively:

$$x + 1/2\ (Da)\ x^2 = t/t_L \qquad (52)$$

$$\frac{\theta_L}{\tau_L} = 1 + 1/2\ Da \qquad (53)$$

Where x is the dimensionless coordinate z_i/L, Da is the Damkohler number $k'L/D_{eA}$, and τ_L is the time constant for leaching given by:

$$t_L = L \frac{f_B\ \rho_B}{k' C_{AO}} = \frac{L^2 \rho_B f_B}{Da\ C_{AO} D_{eA}} \qquad (54)$$

t/τ_L is the dimensionless time for acid attack.

Equations (50) and (52) predict that the interface will retreat rapidly at the start (at small z_i and x) when transport of acid is reaction controlled (small Da), but subsequently more slowly as the reaction becomes diffusion

controlled (large Da). When transport is reaction controlled, equations (50) and (52) become, respectively, equations (55) and (56):

$$z_i = \frac{k' C_{AO}}{\rho_B f_B} t \tag{55}$$

$$x = t/\tau_L \tag{56}$$

Since the Damkohler number is small when transport is reaction controlled, equation (51) indicates that θ_L and τ_L can be used interchangeably in equation (56).

When the reaction is diffusion controlled, equations (50) and (52) become respectively, equations (57) and (58):

$$z_i - z_i^* = \left[\frac{2\, C_{AO}\, D_{eA}}{\rho_B\, f_B}\right]^{1/2} (t-t^*)^{1/2} \tag{57}$$

$$x - x^* = \left[\frac{t - t^*}{\tau_L\, D_A}\right]^{1/2} \tag{58}$$

where $x^* = z_i^*/L$ is the dimensionless interface position at time t^*, when the reaction switches from reaction to diffusion control. This time is somewhat arbitrary since there is no precise criterion which predicts when it will occur. Also, there will be an intervening period during which neither reaction nor diffusion are rate controlling. The duration of this period will depend on the magnitude of

the Damkohler number. At low values the switch will occur at later dimensionless times, while at high values of Da it will occur sooner. As the Damkohler number becomes larger, x* and t' both approach zero and transport becomes diffusion controlled, as indicated by equation (59):

$$z_i = \left[\frac{2\ C_{AO}\ D_{eA}}{\rho_B\ f_B}\right]^{1/2} t^{1/2} \qquad (59)$$

The functional form given in equation (59) agrees with an empirical model previously presented by Turriziani [16] for the progression of a carbonation front through concrete. However, in his model only an empirical (rather than a theoretical) proportionality constant was identified.

Model constants can be determined by a suitable linearizing equation. For reaction control, the linearizing plot is z_i vs. t according to equation (56), while for diffusion control it is $z_i - z^*$ vs. $\sqrt{t-t^*}$ according to equation (57), or just z_i vs $\sqrt{t}$ after equation (59). Equation (50), which encompasses all cases, can also be linearized to give:

$$z_i = \frac{2\ D_{eA}\ C_{AO}}{\rho_B\ f_B} \left(\frac{t}{z_i}\right) - \frac{2\ D_{eA}}{k'} \qquad (60)$$

Here the linearizing plot is z_i vs. t/z_i. The slope of such a plot is $2\ D_{eA}\ C_{AO}/\rho_B\ f_B$, while the intercept is $-2\ D_{eA}/k'$, The best values of the slope and intercept can be found from

a linear least square fit of this equation to the data. A good fit of the data to this equation can supply partial validation of the model. Equation (60) suffers from the problem of plotting a variable against itself, in this case making the data appear to have more error than it really does, especially at early times. From the best slope and intercept the Damkohler number Da and the system time constants R_L and t_L can be found. Use of equation (60) avoids the problem of having to choose an arbitrary cutoff time t* where reaction control ends and diffusion control begins. However, random errors in the data which may be distributed normally in z vs. t data are no longer so distributed when plotting z_i vs. t/z_i. Such problems in data analysis can be mitigated by using a non-linear least squares technique which finds the equation (60) model constants by minimizing (z_i, t) data residuals directly equation (60). Use of these methods of data analysis can help refine the experimental design.

An alternative scenario to that represented by the equations of this section, retains the concept of a sharply moving interface but utilizes the transient concentration profiles $C_A(z,t)$ previously developed and presented in Tables 6 and 7, rather than a strictly quasi-steady-state analysis. Mathematically this would involve finding the concentration gradients $(\partial C_A/\partial z)_{z=z_i}$ needed for substitution into equation (47) from the equations of Table 6 and then integrating as

before to find $z_i(t)$. Although conceptually simple this procedure would be numerically complicated since infinite summations would appear in the integrals. Suitable criteria could be developed to predict the conditions under which these solutions for $z_i(t)$ would reduce to equation (50).

In addition to these considerations, the effect of alternative processes on the prediction of leaching rates should be examined. The most important of these, which has not yet been examined, is convection or flow caused by hydraulic gradients across the slab. The effect of flow on the penetration of sulfate ions into concrete is presented in the following section. The results developed there can be modified to examine the effect that flow has on the rate of acid attack.

4.3 Sulfate Attack

Many of the conceptual and mathematical models that have been developed for chloride diffusion, leaching and acid attack can be applied to the problem of sulfate attack. However, the chemistry of sulfate attack is more complicated. In groundwater and clayey soils, sulfates of sodium, potassium, calcium and magnesium can be naturally present. They can also become concentrated in soils by evaporation or repeated irrigation cycles. Degradation

of concrete by sulfate attack can involve cracking and disintegration, affecting both the integrity and strength of concrete.

Sulfate attack can be accelerated in several ways. Alternate cycles of wetting and drying can concentrate soluble sulfates underneath the exterior faces of concrete members. Hydraulic flow of sulfate solutions from the exterior can augment inherently slow diffusion processes of sulfate ions. Cracking also can significantly increase the diffusion rate since both the void space and connectivity of the pore structure are increased.

4.3.1 Reactions

Reactions between sulfate ions and the constituents of portland cement can occur in both fresh and mature cement pastes. In fresh portland cement paste tricalcium aluminate reacts with interground gypsum and water to form ettringite:

$$3CaO\cdot Al_2O_3 + 3(CaSO_4\cdot 2H_2O) + 26H_2O \rightarrow 3CaO\cdot Al_2O_3\cdot 3CaSO_4\cdot 32H_2O \quad (61)$$

Gypsum is added to portland cement clinker to control the rapid reaction between tricalcium aluminate and water which otherwise could lead to flash set. The ettringite projects a net of long, thin crystalline needles into the pore

solution creating a diffusion barrier which slows the hydration reactions at early ages.

Insufficient gypsum is added to portland cement to consume all the tricalcium aluminate. At later ages, hydration slows to a rate at which flash set is no longer a problem. The volume of ettringite formed is much greater than that of the solid reactants. However, in fresh paste, which has a high porosity, there is often sufficient void space to accommodate growing ettringite needles. Also, the matrix of fresh portland cement paste is not rigid and it can adjust to compensate for internally induced stress. At low concentrations of sulfate ion, the ettringite will transform to monosulfate ($3CaO \cdot Al_2O_3 \cdot CaSO_4 \cdot 12H_2O$).

Hardened portland cement pastes can also react with sulfate ions which intrude into the concrete. Depending upon the environment, at least three major deleterious reactions are known to take place. These include the formation of gypsum from calcium hydroxide and soluble sulfates (equation (62)) ettringite formation (equation (63)), and the reaction of cement gel with magnesium sulfate, (equation (64)) [24,27].

$$2(3CaO \cdot Al_2O_3 \cdot 12H_2O) + 3(Na_2SO_4 \cdot 10H_2O) \rightarrow 3CaO \cdot Al_2O_3 \cdot 3CaSO_4 \cdot 32H_2O + 2Al(OH)_3 + 6NaOH + 16H_2O \quad (62)$$

$$Ca(OH)_2 + Na_2SO_4 \cdot 10H_2O \rightarrow CaSO_4 \cdot 2H_2O + 2NaOH + 8H_2O \quad (63)$$

$$3CaO \cdot 2SiO_2 + 3\ MgSO_4 + 5H_2O \rightarrow 3CaSO_4 \cdot 2H_2O +$$
$$3Mg(OH)_2 + 2SiO_2 \cdot nH_2O \qquad (64)$$

Ettringite can form once gypsum is formed according to equation (63). As in fresher pastes, at low concentrations of sulfate, ettringite will transform to monosulfate with a significant reduction in molecular volume so that cracking may not occur. The local concentration of sulfate ions will determine the ratio of ettringite to monosulfate and thus the propensity for cracking. The local ion concentration will depend on the external concentration of sulfate, the distance to the reaction sites, and the rate of ettringite formation and transformation to monosulfate.

As shown by equation (62) soluble sulfate reacts with the calcium hydroxide in hardened cement paste. The gypsum which forms has a larger molar volume than calcium hydroxide. The formation of gypsum may result in the production of expansive stresses. A similar reaction can occur between calcium hydroxide and magnesium sulfate. Magnesium sulfate can also attack the calcium silicate hydrate directly as indicated by equation (64). Magnesium hydroxide precipitates and the reaction continues until either the calcium silicate hydrate or the magnesium sulfate is consumed. Fortunately, the reaction is slow and external concentrations of magnesium sulfate are generally small

except in soils which have previously been exposed to seawater intrusions. The gypsum formed can be transformed to additional ettringite by reaction with tricalcium aluminate. This process can self-propagate, because as gypsum is consumed in the formation of ettringite via equation (61), the equilibria for both equations (62) and (64) will be shifted towards the product side.

4.3.2 Conceptual Models

Previously developed conceptual and mathematical models [28,29] have focused on the reactions of tricalcium aluminate with interground gypsum rather than the intrusion of sulfate ions from the outside environment. In these models the first stage of the hydration of tricalcium aluminate is controlled by the diffusion of sulfate or aluminate ions through a thickening ettringite layer around tricalcium aluminate particles. During the second stage, which starts when the gypsum has been consumed and sulfate ion concentrations have fallen to low levels, the ettringite dissolves and monosulfate crystals are formed:

$$3CaO\cdot Al_2O_3\cdot 3CaSO_4\cdot 32H_2O + 2(3CaO\cdot Al_2O_3) + 4H_2O \rightarrow 3(3CaO\cdot Al_2O_3\cdot CaSO_4\cdot 12H_2O) \quad (65)$$

In the process of this reaction additional tricalcium aluminate and water are consumed. The second stage has been shown to be controlled by the diffusion of tricalcium aluminate species through a thinning ettringite barrier layer [29]. During the third or last stage, after all the ettringite has been consumed, the surfaces of the remaining unreacted tricalcium aluminate particles are exposed to the pore water. Additional hydration products form around tricalcium aluminate particles, such as cubic and hexagonal hydrates. It appears that the diffusion of water through these hydrates to the tricalcium aluminate surface is the rate controlling step for the last stage [30].

Because of the somewhat different pore solution chemistry in cement systems as compared to the pure tricalcium aluminate-gypsum system, the rates and even mechanisms of these three stages may differ, and care must be exercised in extrapolating results. Nevertheless, it seems that diffusion of ions through product layers is a dominant transport mechanism in both portland cement and tricalcium aluminate systems.

Studies performed by the Building Research Establishment in England [31] on the depth of penetration of sulfate ion into concrete exposed for up to 5 years to groundwater containing sulfate salts show that when a 0.19 M sulfate solution consisting of mixtures of alkali and magnesium sulfates is

used, an interface moved into the concrete at a linear rate. The depth of deterioration z_i (mm) followed the empirical equation:

$$z_i = 5.5\ f_A\ ([Mg] + [SO_4])\ t \qquad (66)$$

where t is the time in years, f_A is the weight fraction of tricalcium aluminate, and [Mg] and [SO_4] are the molar concentrations of magnesium and sulfates, respectively, in the original solutions. Although this empirical relation was only accurate to within 30 percent when compared to accelerated test data, it does suggest that the process was reaction rather than diffusion controlled. Note that equation (66) has a similar functional form to equation (55) which predicts reaction control, rather than equation (57) which describes diffusion control. Although equation (66) is specific for the test conditions employed, reaction control is consistent with a mechanism in which cracking has increased the permeability of the deteriorated concrete to the point where diffusion to the reaction front is significantly increased. The direct dependence of interface depth on the fraction of tricalcium aluminate is inconsistent with equation (55) which predicts an inverse relation. Enhanced cracking that occurs with more reaction is a possible reason for the observed behavior.

4.3.3 Mathematical Models

4.3.3.1 Leaching of Gypsum

Leaching of gypsum occurs by groundwater leaching. The driving force for leaching is the concentration gradient between the inside of the pores and the external groundwater. Mathematical models for sulfate attack can be similar in form to those for chloride intrusion and acid attack. For example, consider the leaching of gypsum from the pores of a slab. The gypsum will be in equilibrium with the local pore water, with an equilibrium sulfate ion concentration represented by C_s^*. If the groundwater outside the slab is sulfate free, then the following equation is applicable:

$$z_i = \left[\frac{2\, D_{es}\, C^*_s\, t}{f_g\, \rho_g}\right]^{1/2} \qquad (67)$$

where D_{es} is the effective diffusion coefficient of sulfate ion, f_g is the volume fraction of the concrete phase occupied by gypsum and ρ_g is the molar density of gypsum. This equation is analogous to equation (59) for the acid attack of calcium hydroxide. Equation (67) predicts that the gypsum interface will slowly retreat into the slab. For this diffusion controlled process, the rate of movement will slow with time. Thus, with diffusion control, it will take

four times as long for the interface to advance to a depth of 2mm as to advance the first millimeter. One would expect leaching by this mechanism to occur quite slowly because not only is D_{es} low but so is C^*_s.

It is also possible to have a dissolution controlled process in which, because of cracking, movement of sulfate ion within the slab is relatively rapid. In this case the concentration of sulfate ions, from the dissolution of gypsum, may be relatively uniform through the whole slab and, therefore, there will be no moving interface. Leaching of sulfate ions will occur through boundary layers on the outside of the slab at a rate controlled by the external groundwater flow. Increases in the flow rates will reduce the thickness of the mass transfer boundary layer and increase the transport of dissolved sulfate ions out of the slab. With constant groundwater flow, the leaching process in this scenario will essentially occur at a constant rate until all the gypsum is dissolved. Leaching by dissolution control is likely to be much more rapid than leaching by diffusion control.

4.3.3.2 Model for Sulfate Attack

Figure 6 shows the model system for sulfate attack of concrete. The outside surface of the slab is presumed to be uniformly exposed to groundwater flow which contains a soluble sulfate salt, such as sodium sulfate. Concrete of intermediate age will contain cement paste with a little unreacted tricalcium aluminate as well as monosulfate which can react to form more ettringite. In mature hardened cement pastes there will be little or no unreacted tricalcium aluminate and the monosulfate can be directly converted to additional ettringite in the presence of soluble sulfate salts.

$$3[CaO\cdot Al_2O_3 \cdot CaSO_4\cdot 12H_2O] + 3Na_2SO_4 \rightarrow 2[3CaO\cdot Al_2O_3 \cdot 3CaSO_4\cdot 32H_2O] + 2\ Al(OH)_3 + 6\ NaOH + 21\ H_2O \qquad (68)$$

Because the products of reaction are more voluminous than the reactants, the formation of ettringite may induce local stresses which cause cracking. Cracking will expose additional monosulfate as well as any unreacted tricalcium aluminate, to the sulfate ions. This can augment sulfate transport so that cracking perpetuates itself.

In the present formulation convection, reaction, and diffusion are considered to be the important transport processes. Figure 6 shows the model system for sulfate attack of concrete. Convection is taken to be in the same

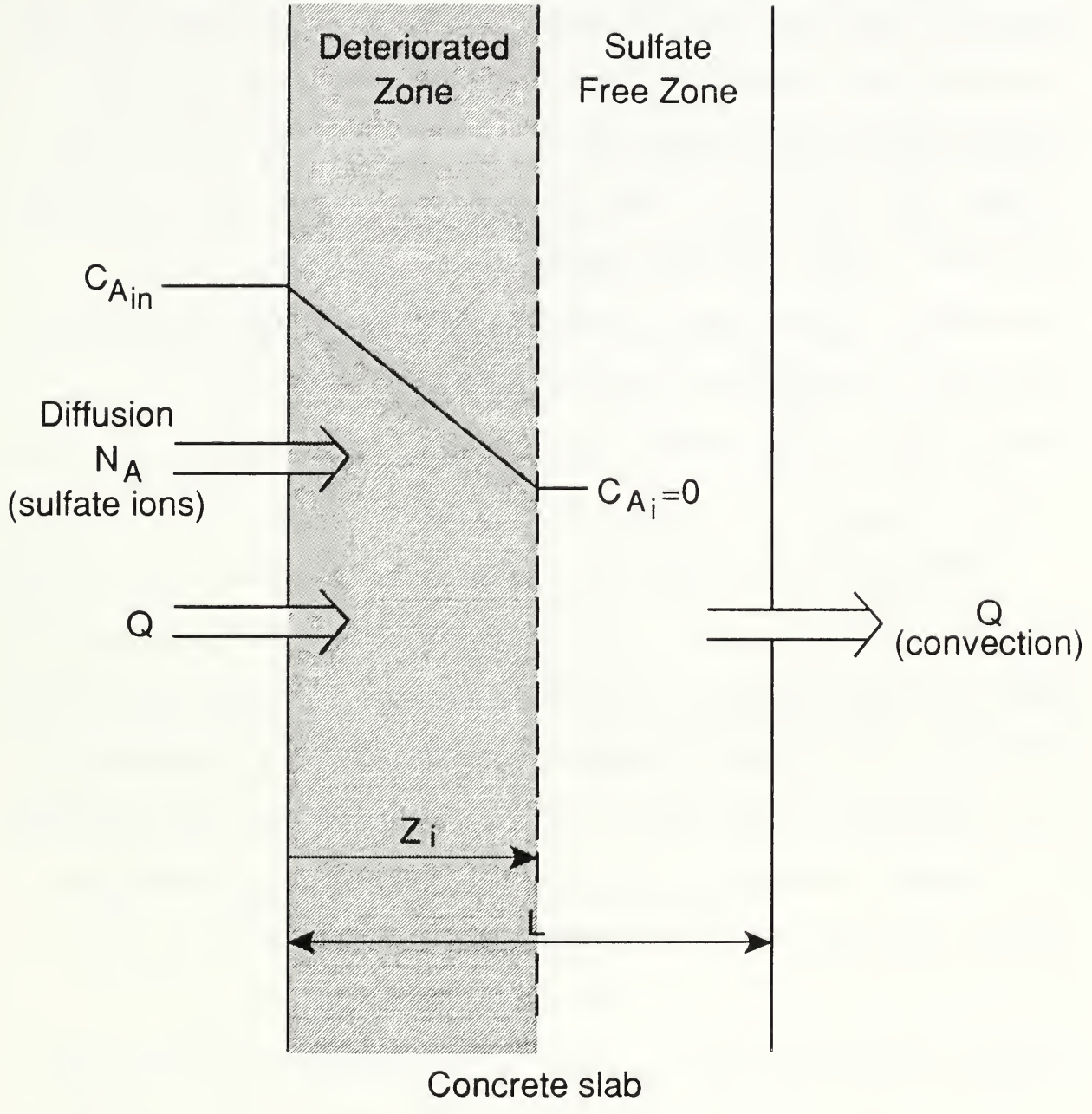

Figure 6. Model system for sulfate attack of concrete: co-current flow.

direction (co-current flow) as diffusion. Diffusion and flow are presumed to occur in only the z direction, which is normal to the face of the slab. It is presumed that at the reaction front reaction occurs rapidly so that C_{Ai}, the concentration of sulfate ion at the interface, is low. A sulfate ion balance is made on a thin element of the slab of thickness dz and constant cross sectional area. The formulation incorporates both the diffusive and convective rate laws, as expressed by equations (5) and (7), respectively. The result is:

$$D_{eA} \frac{d^2C_A}{dz^2} - \epsilon v \frac{d C_A}{dz} = 0 \qquad (69)$$

where ϵ is the porosity of the deterioration zone (0 to z_i) and v is the average velocity of flow based on the total cross section of the slab. In this formulation the porosity is presumed constant at its average value. The effective diffusivity D_{eA} can be estimated from equation (6). Equation (69) can also be obtained more directly as a subcase of equation (18). The first term in equation (69) represents the net diffusion of sulfate ion into the slab element and the second term the net convection. The diffusion time t_d will be small because the diffusion path length z_i is short. Under this condition quasi-steady state will be rapidly attained and then maintained. Under quasi-

steady state conditions there is no accumulation of sulfate ion, and the right hand side of the equation becomes equal to zero.

Equation (69) is subject to two boundary conditions; one at z=0 and one at z_i. These are $C_A(0) = C_{Ain} = C_{A0}$ and $C_A(z_i) = C_{Ai} = 0$, respectively. Presuming that the soil surrounding the slab is much more permeable than the concrete, C_{Ain} can be set equal to C_{AO}. Setting $C_{Ai} = 0$ means that the reaction is so rapid that the sulfate ion concentration is completely consumed at the reaction front. The current model also presumes that there is no overall dimensional change due to expansion, that is, that the total length of the slab remains constant. In practice, sulfate expansion can lead to overall length changes [32]. Solving equation (68) with the prescribed boundary conditions:

$$\frac{C_A}{C_{AO}} = \frac{\exp\left[\epsilon v z / D_{eA}\right] - \exp\left[\epsilon v z_i / D_{eA}\right]}{1 - \exp\left[\epsilon v z_i / D_{eA}\right]} \qquad (70)$$

A quasi-steady state analysis equates the flux of sulfate ions into the slab to the amount of sulfate which is consumed at the moving interface:

$$N_A = - D_{eA} \left(\frac{\partial C_A}{\partial z}\right)_{z=z_i} = \rho_M f_M \frac{dz_i}{dt} \qquad (71)$$

where ρ_M is the molar density of the monosulfate and f_M is its volume fraction in the concrete. The value of f_M can be estimated for hardened cement paste by assuming that all the tricalcium aluminate in the cement has been converted to monosulfate. Equation (70) is consistent with the stoichiometry of ettringite formation (equation (63)) since two moles of sulfate ion reacts with one mole of monosulfate. Substituting equation (69) into equation (70), integrating the resulting differential equation, and writing the result in dimensionless form gives:

$$\exp[-(Pe)\ x] - 1 + (Pe)\ x = (Pe)^2\ t/\tau_S \tag{72}$$

where (Pe) is the Peclet number, $\epsilon vL/D_{eA}$, x is the dimensionless coordinate z_i/L and τ_S is the time constant for sulfate attack given by:

$$\tau_S = \frac{L^2}{D_{eA}} \frac{f_M\ \rho_M}{C_{AO}} \tag{73}$$

t/τ_S is a dimensionless time for sulfate attack.

Equation (71) predicts the location of the interface at any value of time. In this and subsequent formulas the Peclet number (Pe) is to be considered positive regardless of flow direction.

In countercurrent flow, a flow of sulfate-free water opposes the diffusion of sulfate ion into the slab. In this case, equation (73) predicts the location of the interface as a function of time:

$$\exp [(Pe)\ x] - 1 - (Pe)\ x = (Pe)^2\ t/t_s \qquad (74)$$

Equation (73) follows directly from equation (71). The time for the interface to pass completely through the slab θ_s is given by equations (74) and (75) for co- and countercurrent flow, respectively:

$$\theta_{s1} = \tau_s \frac{\exp [-(Pe)] + (Pe) - 1}{(Pe)^2} \qquad (75)$$

$$\theta_{s2} = \tau_s \frac{\exp [(Pe)] - (Pe) - 1}{(Pe)^2} \qquad (76)$$

Here the subscript "s1" denotes co-current flow, while the subscript "s2" denotes counter-current flow.

Diffusion control occurs as Pe → 0. In this case the co-current and countercurrent formulas both reduce to:

$$z_{io} = \left[\frac{2C_{AO}\ D_{eA}}{f_M\ \rho_M}\right]^{1/2} t^{1/2} \qquad (77)$$

$$\theta_{so} = 1/2\ \tau_s \tag{78}$$

Here the subscript "o" denotes no convection.

Equation (76) agrees with equation (59), the diffusion controlled limit solution for acid attack. As shown by equation (77) equations (74) and (75) both reduce to $\theta_s = \tau_s/2$ as Pe $\rightarrow$ 0.

Using the above relations it can be shown for the same Peclet number and time constant that the deterioration interface has moved in faster for co-current flow than for countercurrent flow. In addition, $\theta_{s2} > \theta_{s1}$. These results agree with intuition, since diffusion is slowed when the molecules must move upstream against the opposing flow. When flow opposes diffusion, it will take much longer for the interface to penetrate the slab, thereby extending the service life. For example when (Pe) = 1 the values of θ_{s2}, θ_{s0} and θ_{s1} are in the ratio 1.44 to 1 to 0.72, where θ_{s0} has been taken equal to unity for comparison purposes. These calculations and others establish that, for the same Peclet number, countercurrent flow acts to extend service life more than co-current flow acts to shorten it. This result suggests that it would be advantageous, if possible, to permanently pressurize the inside of containment vessels intended for storing low-level nuclear wastes.

The deteriorated zone of the concrete should have a higher porosity and permeability than the intact concrete. Thus, it would be expected that for the same hydraulic gradient across the concrete, that the flow rate and thus the Peclet number will increase over time. This will help extend the service life with countercurrent flow, but will reduce it with co-current flow, since higher Peclet numbers will carry sulfate and other deleterious ions deeper into the pore structure.

5. SUMMARY AND CONCLUSIONS

With the aim of predicting the service life of concrete intended for use as a disposal facility for low-level nuclear wastes, conceptual and mathematical models have been developed for the intrusion of chemical species into concrete. In the development of the conceptual models, the method of dimensionless groups was used to determine the relative importance of the possible rate controlling processes. Using the method of dimensionless groups, it was shown for moderate to low pressure or hydraulic gradients to which the concrete was subject, that flow or convection was not likely to be as important a mode of transport of deleterious chemical species as diffusion. However, the presence of even a small number of contiguous microscopic cracks through the concrete structure is enough to make such a conclusion invalid. Transient or unsteady state effects

were assessed using the same methods. Because of the small diffusivities of ions through mature hardened cement pastes it is possible for these effects to be important for years. This can provide an additional measure of protection and appreciably extend service life, especially for thick-walled structures.

Phenomena modeled included diffusion, convection, and reaction and sorption. Rate laws were written for these processes and substituted into the conservation equations for chemical species. The resulting differential equations were written in both dimensional and dimensionless terms, and the different kinds of initial and boundary conditions to which they are subject were identified and compared. The independent variables of the model were position and time, and the dependent variables were concentration and molar flux of chemical species.

This general formulation was applied to three specific systems: the penetration of chloride ions, leaching by acid attack, and the penetration of sulfate ions in concrete. After the chemistry and physics of these processes were reviewed, models for each of these processes were developed as separate subcases of the general model.

The model system consisted of a flat slab of concrete whose exterior face was suddenly exposed to a hostile environment.

The models were solved analytically to predict the concentration profiles within the concrete and, in some cases, the location of the reaction front or thickness of the deterioration zone. In most cases, for generality, the solutions were presented in terms of dimensionless variables. For chloride ion intrusion, the concentrations varied with both time and position within the slab as a result of diffusion and reaction or sorption. Reactions occurring between chloride ion and hydrated tricalcium aluminate to form chloraluminates were considered. The key dimensionless group in the analysis was the Thiele modulus, m, which measured the relative importance of reaction to diffusion. Both long and short time model solutions were obtained as well as limit forms when reaction or diffusion only were significant. At both very short and very long dimensionless times the solutions for chloride ion concentration reduced to those previously reported in the literature.

The model for acid attack involved the penetration of dissolved carbon dioxide, carbonic acid or bicarbonate ion into the slab to react with alkali hydroxides and calcium hydroxide. This reaction established a carbonated zone that slowly moved into the slab. Both reaction and diffusion were considered to be potentially important phenomena. The key dimensionless group in the analysis is the Damkoler number Da which, like the Thiele modulus, is a measure of

the relative importance of reaction to diffusion. At low values of Da, acid attack was reaction controlled and the carbonated zone was predicted to move in linearly with time. At high values of Da, reaction was diffusion controlled and the interface was predicted to move in at a rate which slowed with time. This last model agreed in functional form with a previously reported empirical model in the literature.

The model developed for sulfate attack also involved a moving interface between a porous or cracked ettringite layer on the outside of the slab and a relatively impermeable layer of concrete containing monosulfate on the inside. At the moving front, soluble sulfate, brought in from the outside by diffusion and convection, reacted rapidly with the monosulfate to form ettringite. Convection or flow is caused by pressure or hydraulic gradients across the slab in either direction. Flow in the same direction as diffusion (co-current flow) provided a leaching action. The key dimensionless group in the analysis was the Peclet number which measures the relative importance of convection to diffusion. At low values of the Peclet number, reaction was predicted to be diffusion controlled and the deterioration zone followed the same equation as for diffusion controlled acid attack. At high values of the Peclet number, corresponding to convection or leach-rate control, the zone was predicted to move in more rapidly with

co-current flow of groundwater, while with countercurrent flow of sulfate free groundwater, the interface moved in at a much slower rate than if there were no flow.

It is important to emphasize that the model solutions presented in this report are not exhaustive nor are they necessarily unique to the application considered. Thus, the models developed for chloride intrusion, acid attack and sulfate have a degree of interchangeability. Model validity can only be determined by comparing competing models to experimental observation. Once the models and mechanisms on which they are based have been validated, model solutions can form a basis for predicting the life of concrete under in-service conditions.

6. REFERENCES

1. J. R. Clifton and L. I. Knab, "Service Life of Concrete," NISTIR 89-4086, National Institute of Science and Technology, June (1989).

2. J. Pommersheim and J. Clifton, "Mathematical Modeling of Tricalcium Silicate Hydration," Cement and Concrete Research, 9, 765 (1979).

3. E. E. Petersen, Chemical Reaction Analysis, Prentice-Hall (1965).

4. R. B. Bird, W. E. Stewart and E. N. Lightfoot, Transport Phenomena, John Wiley & Sons (1960).

5. A. Kumar, "Diffusion and Pore Structure Studies in Cementitious System," Ph.D. Thesis, Penn State University (1985).

6. F. A. L. Dullien and G. K. Dhawan, J. Colloid Interface Sci., 52, 129 (1975).

7. F. A. L. Dullien, "New Network Permeability Model of Porous Media," AIChE J., 21 (2), 299-307 (1978).

8. H. S. Fogler, Elements of Chemical Reaction Engineering, Prentice-Hall (1986).

9. D. A. G. Bruggeman, Ann. Physik, 24, 636 (1935).

10. D. M. Young and A. D. Crowell, Physical Adsorption of Gases, Butterworths (1962).

11. O. Levenspiel, Chemical Reaction Engineering, 2nd ed., John Wiley & Sons, Inc. (1972).

12. P. V. Danckwerts, "Continuous Flow Systems Distributions of Residence Times," Chem. Eng. Sci., 2, 1 (1953).

13. I. Biczok, Concrete Corrosion and Concrete Protection, Chemical Publishing Co., Inc., New York (1967).

14. K. Tuutti, "Corrosion of Steel in Concrete", Swedish Cement and Concrete Research Institute, Stockholm (1982).

15. "Corrosion of Metals in Concrete," ACI Journal, 3-32, January-February (1985).

16. R. Turriziani, "Internal Degradation of Concrete: Alkali-Aggregate Reaction, Reinforcement Steel Corrosion," 8th International Symposium on Chemistry of Cement, Vol. 1, 388-442, Rio de Janeiro, (1986).

17. R. Aris, The Mathematical Theory of Diffusion and Reaction in Permeable Catalysts, Vol. 1, The Theory of the Steady State, Oxford: Clarendon Press (1975).

18. A. Atkinson and A. K. Nickerson, "Diffusion and Sorption of Cs, Sr and I in Water-Saturated Cement," Report AERE-R 12124, Materials Development Division, Harwell Laboratory, Oxfordshire (1986).

19. C. D. Lawrence, "Durability of Concrete: Molecular Transport Processes and Test Methods," Technical Report 544, Cement and Concrete Association (1981).

20. A. Atkinson, "The Time Dependence of pH within a Repository for Radioactive Waste Disposal," Report AERE-R 1177, Materials Development Division, Harwell Laboratory, Oxfordshire (1985).

21. L. A. Zarra, "The Mathematical Modeling of Portland Cement Hydration," Masters Thesis, Bucknell University (1986).

22. F. M. Lea, The Chemistry of Cement and Concrete, 3rd ed., Chemical Publishing Co., Inc., New York (1971).

23. W. F. Langelier, Journal of the American Water Works Association, 23, 1500 (1936).

24. W. C. Hanson, The Chemistry of Sulphate-Resisting Portland Cements, E. G. Swenson (ed.), University of Toronto Press (1968).

25. R. C. Reid, J. M. Prausnitz and T. K. Sherwood, The Properties of Gases and Liquids, (3rd ed.), McGraw-Hill (1977).

26. J. M. Pommersheim, "Spherical Phase Change with First Order Chemical Reaction," 82nd National Meeting of AIChE, Atlantic City, September (1976).

27. A. M. Neville, Properties of Concrete, 3rd ed., Pitman Publishing Lts., London, (1981).

28. P. W. Brown et. al., "The Hydration of Tricalcium Aluminate and Tetracalcium Aluminoferrite in the Presence of Calcium Sulfate," RILEM, Journal of Materials and Structure, 19 (110), 137-148 (1986).

29. J. Pommersheim and J. Chang, "Kinetics of Hydration of Tricalcium Aluminate in the Presence of Gypsum," Cement and Concrete Research, 18, 911-922 (1988).

30. J. Pommersheim and J. Chang, "Kinetics of Hydration of Tricalcium Aluminate," Cement and Concrete Research, 16, 440-450 (1986).

31. A. Atkinson, D. J. Goult and J. A. Hearne, "An Assessment of the Long-Term Durability of Concrete in Radioactive Waste Repositories," Mat. Res. Soc. Symp. Proc., Vol. 50, 239 (1985).

32. "Standard Test Method for Potential Expansion of Portland-Cement Mortars Exposed to Sulfate", ASTM Designation: C452-89, American Society for Testing and Materials (1989).

33. "Standard Test Method for Length Change of Hydraulic-Cement Mortars Exposed to a Sulfate Solution," ASTM Designation: C1012-89, American Society for Testing and Materials (1989).

7. NOTATION

a	-	stoichiometric coefficient
A	-	acid, or other reactant
b	-	stoichiometric coefficient
B	-	base, or other reactant
C	-	dimensionless concentration
C_A	-	concentration of A
C_{Ai}	-	interfacial concentration of A
C_{Ain}	-	concentration of A in upstream reservoir
C_{AL}	-	concentration of A at slab exit (z=L)
C_{AO}	-	concentration of A next to slab surface (z=0)
C_{Aout}	-	concentration of A in downstream reservoir
$C_A(z,t)$	-	concentration of A at depth z and time t
C_B	-	concentration of B
C^*_B	-	saturation (equilibrium) concentration of B
C_i	-	dimensionless concentration of species i
C_{in}	-	dimensionless concentration of C_{Ain}
C_L	-	dimensionless concentration at z=L
C_O	-	dimensionless initial concentration
C_{OA}	-	initial concentration of A
C^*_S	-	saturation (equilibrium) sulfate concentration
CSH	-	calcium silicate hydrate
D	-	free stream diffusivity
D_A	-	free stream diffusivity of A
Da	-	Damkohler number (also m^2)
D_a	-	apparent diffusion coefficient
D_e	-	effective diffusion coefficient
D_{eA}	-	effective diffusion coefficient of A
D_{eS}	-	effective diffusion coefficient of sulfate ion
E	-	chemical activation energy
erfc	-	complementary error function
F_A	-	molar flow rate of A
f_A	-	weight fraction of tricalcium aluminate
f_B	-	volume fraction of B
f_g	-	volume fraction of gypsum
f_M	-	volume fraction of monosulfate
g	-	ratio of free concentration to total concentration
HCP	-	hydrated cement paste
k	-	reaction velocity constant
K_a	-	adsorption equilibrium constant
k_a	-	adsorption rate constant
k_d	-	desorption rate constant
K_r	-	thermodynamic reaction equilibrium constant
k_1	-	forward reaction velocity constant
k_2	-	reverse reaction velocity constant
k'	-	reaction velocity constant, modified leaching rate constant (kC_B^*)
K_∞	-	equilibrium constant at very high temperature
k_∞	-	rate constant at very high temperature
L	-	thickness of slab
LLW	-	low level nuclear waste
m	-	kinetic order of reaction, Thiele modulus

m^2 - Damkohler number (also Da)
M_{AL} - total moles of A moving completely through slab
M_{AO} - total moles of A penetrating into slab
MIP - mercury intrusion porosimetry
N_A - molar flux of diffusion specie A
P - absolute pressure
Pe - Peclet number
Q - volumetric flow rate (convective)
QSS - quasi-steady state
R - ideal gas law constant, particle radius
r - pore size (radius)
r_A - sorption or reaction rate of A
r_d - dimensionless reaction rate
r* - critical pore radius
S - cross sectional area of slab
S_g - specific surface area of pores
T - absolute temperature
t - time
t_c - time constant for convection
t_d - time constant for diffusion
t_o - initiation time of $Ca(OH)_2$ leaching
t' - dimensionless time
t* - time when process switches from reaction to diffusion control
u - stoichiometric coefficient, variable of integration
U - reaction product
V - volume
v - average flow velocity
V_g - specific pore volume
w - thickness of reaction rim
w/c - water-to-cement ratio by weight
x - dimensionless distance
y - stoichiometric coefficient
Y - reaction product
z - distance, thickness
z_i - distance of interface from slab surface
z_{io} - value of z_i if Pe = 0
z_i* - value of z_i when t=t*
z' - dimensionless z_i

ΔC - concentration difference
∇C - concentration gradient
ΔH - energy of reaction or sorption
ΔP - pressure difference across slab
ρ_B - molar density of B
ρ_g - molar density of gypsum
ρ_M - molar density of monosulfate
ϵ - flow porosity
μ - absolute viscosity
σ - constriction factor
τ_L - time constant for leaching
τ_s - time constant for sulfate attack
τ - tortuosity

θ - total time
θ_s - time for interface to pass through slab (sulfate attack)
θ_{s0} - value of θ_s if Pe = 0
θ_{s1} - value of θ_s for co-current flow
θ_{s2} - value of θ_s for countercurrent flow

Peclet number $\epsilon vL/D_e$

Thiele modulus $\left[\frac{k'R^2}{D_e}\right]^{1/2}$ or $\left[\frac{\epsilon k}{D\epsilon A}(S/V)_g L^2\right]^{1/2}$

NIST-114A
(REV. 3-89)

U.S. DEPARTMENT OF COMMERCE
NATIONAL INSTITUTE OF STANDARDS AND TECHNOLOGY

BIBLIOGRAPHIC DATA SHEET

1. PUBLICATION OR REPORT NUMBER
NISTIR 4405

2. PERFORMING ORGANIZATION REPORT NUMBER

3. PUBLICATION DATE
SEPTEMBER 1990

4. TITLE AND SUBTITLE

MODELS OF TRANSPORT PROCESSES IN CONCRETE

5. AUTHOR(S)

James M. Pommersheim and James R. Clifton

6. PERFORMING ORGANIZATION (IF JOINT OR OTHER THAN NIST, SEE INSTRUCTIONS)

U.S. DEPARTMENT OF COMMERCE
NATIONAL INSTITUTE OF STANDARDS AND TECHNOLOGY
GAITHERSBURG, MD 20899

7. CONTRACT/GRANT NUMBER

8. TYPE OF REPORT AND PERIOD COVERED

9. SPONSORING ORGANIZATION NAME AND COMPLETE ADDRESS (STREET, CITY, STATE, ZIP)

10. SUPPLEMENTARY NOTES

[ ] DOCUMENT DESCRIBES A COMPUTER PROGRAM; SF-185, FIPS SOFTWARE SUMMARY, IS ATTACHED.

11. ABSTRACT (A 200-WORD OR LESS FACTUAL SUMMARY OF MOST SIGNIFICANT INFORMATION. IF DOCUMENT INCLUDES A SIGNIFICANT BIBLIOGRAPHY OR LITERATURE SURVEY, MENTION IT HERE.)

An approach being considered by the U.S. Nuclear Regulatory Commission for disposal of low-level radioactive waste is to place the waste forms in concrete vaults buried underground. The vaults would need a service life of 500 years. Approaches for predicting the service life of concrete of such vaults include the use of mathematical models.

Mathematical models are presented in this report for the major degradation processes anticipated for the concrete vaults, which are corrosion of steel reinforcement, sulfate attack, acid attack, and leaching. The models mathematically represent rate controlling processes including diffusion, convection, and reaction and sorption of chemical species. These models can form the basis for predicting the life of concrete under in-service conditions.

12. KEY WORDS (6 TO 12 ENTRIES; ALPHABETICAL ORDER; CAPITALIZE ONLY PROPER NAMES; AND SEPARATE KEY WORDS BY SEMICOLONS)

Acid attack; chloride; concrete; convection; corrosion; diffusion; leaching; mathematical model; service life; sulfate attack; transport processes

13. AVAILABILITY

[X] UNLIMITED

[ ] FOR OFFICIAL DISTRIBUTION. DO NOT RELEASE TO NATIONAL TECHNICAL INFORMATION SERVICE (NTIS).

[ ] ORDER FROM SUPERINTENDENT OF DOCUMENTS, U.S. GOVERNMENT PRINTING OFFICE, WASHINGTON, DC 20402.

[X] ORDER FROM NATIONAL TECHNICAL INFORMATION SERVICE (NTIS), SPRINGFIELD, VA 22161.

14. NUMBER OF PRINTED PAGES
101

15. PRICE
A06

ELECTRONIC FORM